TOWSON UNIVERSITY

OFFICE OF GRADUATE STUDIES

THE DEVELOPMENT OF THE ACADVL SCANNING ASSAY USING A TWO-STEP PCR

AND HIGH RESOLUTION MELTING ANALYSIS

by

Nadia Benkhadra

A thesis

Presented to the faculty of

Towson University

in partial fulfillment

of the requirements for the degree

Master of Science in Forensic Science

Towson University
Towson, Maryland 21252
May 2014

TOWSON UNIVERSITY
OFFICE OF GRADUATE STUDIES

THESIS APPROVAL PAGE

This is to certify that the thesis prepared by Nadia Benkhadra entitled The Development of the
ACADVL Scanning Assay using a Two-Step PCR and High Resolution Melting Analysis
has been approved by the thesis committee as satisfactorily completing the thesis
requirements for the degree Master of Science in Forensic Science in the Department of
Chemistry.

Cynthia Zeller, PhD Chair, Thesis Committee   5/2/14
                                                       Date

Kelly Elkins, PhD Committee Member   5/2/2014
                                                       Date

Leka Papazisi, DVM, PhD Committee Member   5/2/2014
                                                       Date

Dean of Graduate Studies   5/7/14
                                                       Date

i

ACKNOWLEDGEMENTS

ABSTRACT

The Development of the ACADVL Scanning Assay using a Two-Step PCR and High Resolution
Melting Analysis

Nadia Benkhadra

Very long chain acyl-CoA dehydrogenase deficiency is the second most common fatty acid

oxidation disorder detected by newborn screening. Currently, tandem mass spectrometry is used

as the primary detection method, followed by molecular genetic testing to confirm the presence

of a mutation. A simpler, more cost effective method of diagnosis is high resolution melting

(HRM) following amplification of the target. HRM does not require physical processing or

separation steps. In this study, PCR primers' that amplify each of the 20 exons that make up the

ACADVL gene were designed. One primer pair for each exon was selected based on PCR

performance and target specificity. After defining the PCR cycling conditions, we performed a

blinded study with 30 different genomic DNA samples. Synthetic constructs were used as

positive controls for each test. Seven different mutations were detected from the high resolution

melting profiles. Bi-directional DNA sequencing (Sanger Sequencing) confirmed the mutations.

TABLE OF CONTENTS

LIST OF TABLES

LIST OF FIGURES

CHAPTER I

BACKGROUND

The body requires constant sources of fuel to perform every day functions. Its source of energy depends on the availability of certain molecular resources. Two important sources of energy are carbohydrates and fatty acids. Carbohydrates, such as glucose, are an important source of energy in the body, but fatty acids are able to store much more energy per gram (Croston, 2001). They are major sources of energy for the heart and muscle. The brain also uses fatty acids as a source of fuel in addition to glucose and ketone bodies. During periods of fasting, they serve as important energy sources for the liver and other tissues as well. In the adipose tissue, fatty acids are stored in the form of triglycerides, which consist of three fatty acid molecules and one glycerol molecule (Croston, 2001). When glucose levels are low, usually during periods of fasting, glucagon, an enzyme secreted by the pancreas, initiates adipose tissue lipase activity (Croston, 2001). This enzymatic activity triggers the hydrolysis of triglycerides and the release of fatty acids. The "free" fatty acids travel through the blood via albumin and lipoproteins to other tissues such as muscle and are oxidized to provide energy via the mitochondrial beta oxidation pathway. Short and medium chain fatty acids of less than 10 carbons are able to cross the outer and inner mitochondrial membranes to enter the mitochondrial matrix (Tein, 2002). However, the mitochondrial membrane is impermeable to long-chain fatty acids (Tein, 2002). Fatty acid beta oxidation occurs in the mitochondrial matrix, which requires long chain fatty acids to be transported from the cytoplasm of the cell, across the mitochondrial membrane. The transport of long chain fatty acids into the mitochondria is accomplished by the

enzyme carnitine palmitoyl transferase I , which is located on the inner membrane (Croston, 2001) (Tein, 2002).

The beta oxidation pathway is a series of four reactions (**Figure 1**). The first reaction, catalyzed by the enzyme acyl-CoA dehydrogenase, is a dehydrogenation, or oxidation, reaction that introduces a trans C=C bond between the alpha and beta carbons of the fatty acyl CoA molecule using a mechanism that reduces membrane bound FAD to $FADH_2$ (Miesfeld D. , 2008). After oxidation is complete, enoyl-CoA hydratase catalyzes the hydration reaction. This enzyme adds H_2O across the C=C bond to convert trans-delta2-enoyl-CoA to 3-L-hydroxyacyl-CoA. In the third reaction, beta-hydroxyacyl-CoA dehydrogenase removes an electron pair from the substrate and donates it to NAD^+ to form NADH (Miesfeld, 2008). The final step in the beta-oxidation pathway is a thiolysis reaction which is catalyzed by the enzyme acyl-CoA acetyltransferase, also known as thiolase. During this step, a molecule of acetyl-CoA is released and a fatty acyl-CoA product that is two carbons shorter than the starting substrate is produced (Miesfeld, 2008). These reactions occur in repeating cycles with each fatty acid molecule until consumed. During each cycle, the fatty acid molecules are oxidized and shortened by two carbons. The energy released is captured by the reduced carrier molecules NADH and $FADH_2$. At the end of each four reaction cycle, a two-carbon acetyl-CoA molecule is released from the end of the fatty acid. The fatty acid molecule continues through another round of beta oxidation until all even chain fatty acids are oxidized to acetyl-CoA. The number of acetyl-CoA molecules produced depends on the carbon length of the fatty acid being oxidized (Miesfeld, 2008).

Very long chain acyl-CoA dehydrogenase (VLCAD) belongs to a family of acyl-CoA dehydrogenase (ACAD) flavoenzymes that catalyze the alpha-beta-dehydrogenation of acyl-CoA

esters using the electron transfer flavoprotein (ETF) as their electron acceptor. There are four highly homologous, straight chain acyl-CoA dehydrogenase enzymes with differing chain lengths which catalyze this first step: very long chain acyl-CoA dehydrogenase (VLCAD; uses C14-C20 fatty acyl-CoAs), long chain acyl-CoA dehydrogenase (LCAD; uses C10-C14 fatty acyl-CoAs), medium chain acyl-CoA dehydrogenase (MCAD; uses C6-C10 fatty acyl CoAs), and short chain acyl-CoA dehydrogenase (SCAD; uses C4-C6 fatty acyl-CoAs). All acyl-CoA dehydrogenase enzymes, except VLCAD, are mitochondrial matrix associated homotetramers composed of monomers that are nearly identical in size (~40kDa). VLCAD is a homodimer consisting of 70 kDa subunits associated with the inner mitochondrial membrane. It has an additional 180 amino acids at its carboxy terminus which facilitates its interaction with the inner mitochondrial membrane and other fatty acid oxidation proteins (Schiff, et al., 2013).

There are a number of specific enzyme deficiencies associated with fatty acid oxidation, one of which is very long chain acyl-coenzyme A dehydrogenase deficiency (VLCADD). VLCADD is an autosomal recessive inherited disorder that affects the first step in the beta oxidation pathway (Olsen, et al., 2010). In VLCADD, enzymatic deficiency causes the accumulation of long-chain acylcarnitine, with C14:1-carnitine as the disease specific marker (Schymik, et al., 2006). Deficiency in this gene product reduces myocardial fatty acid beta-oxidation and is associated with cardiomyopathy. While the pathology is rather complex, disease can be avoided or reversed with early intense treatment by a simple change in diet. Cox et al. (2008) described the outcome for a 5-year-old girl with VLCAD deficiency that was first seen at 5 months of age with severe hypertrophic cardiomyopathy (Cox, et al., 2008). Molecular genetic analysis revealed two VLCAD mutations. The patient was placed on a low-fat diet supplemented

with medium-chain triglyceride oil and avoidance of fasting (Cox, et al., 2008). Over the course of a year, her ventricular hypertrophy resolved significantly (Cox, et al., 2008). The case study presented by Cox et al. (2008) expressed the importance of early clinical recognition of VLCAD deficiency because it is one of few directly treatable causes of cardiomyopathy in children (Cox, et al., 2008).

Three disease phenotypes associated with VLCADD have been documented. Severe infant onset is characterized by acute metabolic decompensation with hypoketoic hypoglycemia, dicarboxylic aciduria, liver dysfunction and cardiomyopathy. The patients who have survived their initial symptoms exhibit progressive cardiomyopathy and have a reported 75% mortality (Schiff, et al., 2013). The second form of the disease presents later in infancy or early childhood but has a milder phenotype that does not include cardiac involvement (Goetzman, et al., 2007).The third form presents itself in adolescents or adults and is dominated by muscle dysfunction, which is often induced by exercise. Andresen et al. (1999) examined the correlation between the phenotypes and the known VLCAD genotypes associated with the deficiency. They examined 58 different mutations in 55 unrelated individuals. The results of this study showed a clear relationship between the nature of the mutation and the severity of the disease (Andresen, et al., 1999). Patients that presented severe childhood phenotypes have mutations that resulted in no residual enzyme activity, whereas those that displayed the milder childhood and adult phenotype have mutations that may have resulted in residual enzyme activity (Andresen, et al., 1999).

The American College for Molecular Genetics (ACMG) has developed a uniform set of guidelines for newborn screening programs. Five fatty acid oxidation disorders were included in the core panel: medium chain acyl-CoA dehydrogenase deficiency (MCADD); very long chain

acyl-CoA dehydrogenase deficiency (VLCADD); long-chain L-3-OH acyl-CoA dehydrogenase deficiency (LCHADD); trifunctional protein deficiency (TFPD); carnitine uptake defect (CUDD) (Watson, et al., 2006). VLCADD is the second most common enzymatic deficiency that affects the fatty acid oxidation pathway, behind MCADD. MCADD has a higher prevalence of disease compared to VLCADD. Data collected from newborn screening programs suggested a VLCADD prevalence of 1:31,500 to 1:125,000 in Caucasians; whereas MCAD has a suggested prevalence of 1:4,900 to 1:17,000 (Olsen, et al., 2010) (Matern, et al., 2012). However, both MCAD and VLCAD were given high scores based on the ACMG selection criteria for newborn screening programs in part because of the significant health impact genetic conformation tests can yield. Early identification of affected individuals allows simple dietary treatments to be communicated to the parents and started before any significant fatty acid build up occurs in the infant.

Gene Structure and Mutations

VLCAD is encoded by the *ACADVL* gene (OMIM entry: MIM*609575)[1]. It is the only gene in which mutations are known to cause VLCAD deficiency. The VLCAD enzyme also has the following aliases: ACAD6, LCACD, and ACADVL. The gene itself is fairly compact, consisting of 5.4 kilobases (kb) from the presumed transcription start site to poly (A) addition. It is located on the short arm of chromosome 17 at position 13.1 (17p13.1) and contains 20 exons ranging from 63-309 base pairs (bp) in length. Fifty-eight percent of the gene is composed of introns. The largest intron is 459 bp and the smallest is 71 bp. One unique aspect of the *ACADVL* gene is its high GC content. The exon and intron percent GC content are 58% and 61% respectively (Leslie, et al., 2011).

---

[1] http://www.omim.org/entry/609575

According to the Human Genome Mutation Database (HGMD)[2], there are 196 known mutations in *ACADVL*. The HGMD has described 116 of these and 80 have recently been reported in a study explaining gene scanning through high resolution melting (HRM) analysis (Olsen, et al., 2010). The nomenclature used to identify a mutation can be described as follows: "c." stands for the coding DNA; the number corresponds to the nucleotide position; the first letter describes the homozygous wild-type DNA; the second letter describes the homozygous mutant DNA. One of the most common pathological alleles is c.848T>C where amino acid valine is substituted for alanine. The c.848T>C is observed in symptomatic compound heterozygotes and in homozygotes. It makes up about 20% of mutant alleles of the individuals detected by newborn screening. Other frequent mutations include c.779C>T and 830_832del, which are located in close proximity to one another on exon 9.

Current Testing Protocol

VLCADD is currently identified by newborn screening (NBS) of acylcarnitine profiles from plasma or dried blood spots with tandem mass spectrometry followed by molecular genetic testing of *ACADVL*. Tandem mass spectrometry, or MS/MS, uses two mass spectrometers in tandem to determine the molecular structure of analytes. For VLCADD identification, the MS/MS measures C14-C20 straight chain acyl carnitine esters, 3-hydroxy-acyl carnitine esters, and unsaturated acyl carnitine esters. This method is most sensitive during periods of metabolic stress, such as fasting. The C14:1 acylcarnitine is the principle metabolite used to identify VLCADD; however, it does not always discriminate between affected patients and carriers and healthy individuals. Schmyck et al. (2006) analyzed acylcarnitine levels in two patients on day

---

[2] The Human Gene Mutation Database: http://www.hgmd.org/

three of life. The study showed that during the catabolism on day 2 to 3 of life, all transporters and enzymes required for fatty acid beta-oxidation were induced, thereby normalizing the C14:1-carnintine levels in patients with mild VLCADD (Schymik, et al., 2006). Samples that screened positive for the presence of pathological acylcarnitine esters are confirmed through molecular genetic testing. These secondary tests include sequence analysis and deletion/duplication analysis. Sequence analysis, which is a PCR-based approach, involves sequencing all 20 exons and exon/intron boundaries of the gene. This approach has been shown to detect mutations in 85%-93% of individuals with VLCADD. Deletion/duplication analysis is performed if sequencing results did not identify a mutation. The methods used for deletion/duplication detection include quantitative PCR, long-range PCR, probe amplification, or targeted chromosomal microarray analysis (Leslie, et al., 2011).

High Resolution Melting (HRM) Analysis

The melting properties of DNA have assisted in the development of many clinical, genetic and forensic tests (Erali, et al., 2008). As the DNA double helix is heated, the strands separate in a process called denaturation or melting. For short PCR products, the melting occurs in one transition, whereas longer PCR products may melt in multiple stages, also known as melting domains (Erali, et al., 2010). The melting temperature (T_m) of the DNA is dependent on GC content, length and sequence composition, so PCR products can be distinguished by their melting curves (Ririe, et al., 1997). The T_m is defined as the temperature at which half of the duplexes are dissociated (Erali, et al., 2010). It is conventionally monitored by UV absorbance, which requires micrograms of DNA for high quality melting curves. Unlike UV absorbance, monitoring DNA melting with fluorescence is more sensitive and only requires nanograms of

DNA input. This technique is accomplished by incorporating fluorescent dyes into the PCR reaction.

In 1997, fluorescent DNA melting as a companion to real-time PCR was first introduced with the LightCycler instrument (Idaho Technology and Dr. Carl Wittwer's DNA Lab at the University of Utah) (Wittwer, 2010). The implementation of fluorescence-based DNA melting coupled with PCR required no handling, processing, or separation of the sample after amplification. Methods for both probe and amplicon melting were developed and incorporated into the real-time PCR instruments (Wittwer, 2010). Amplicon melting with SYBR Green I (Life Technologies, Inc.) became more popular than the probe based methods primarily because of cost and convenience of PCR product analysis after amplification (Wittwer, 2010). These saturating dyes are a new family of double-stranded DNA binding dyes that allow genotyping by melting without the use of a fluorescently-labeled probe. The dye is highly fluorescent when bound to double-stranded DNA, but it fluoresces poorly in the unbound state. After the target of interest has been amplified, the amplicon is gradually denatured by increasing the temperature in small increments. Initially, any double-stranded DNA that is present will show high levels of fluorescence, and as the temperature increases, the fluorescence will begin to decrease. Then, at a characteristic temperature, the fluorescence rapidly drops **(Figure 2A).** This reflects the melting of DNA into single strands.

The first real-time PCR instruments did not focus on the melting quality of the data produced. In 2000, the Wittwer DNA Lab initiated a project with Idaho Technology to build a high-resolution melting (HRM) instrument. In 2002, the HR-1 instrument was introduced. This instrument used very small sample volumes and capillary tubes instead of a well plate, and dyes

with higher saturation levels were used in the PCR chemistry, enabling HRM to progress (Wittwer, 2010). HRM analysis software packages are used to identify pre- and post-melt fluorescence intensity. The melting temperature (T_m) can be approximated by taking the negative first derivative (-dF/dT) of the melting curve (**Figure 2B**) (Reed, et al., 2007) (Erali, et al., 2008). These signals are automatically normalized to relative values, eliminating differences in background fluorescence (**Figure 2C**). The melting temperature shifts as well as the curve shape are used to identify possible variants. One form of this analysis is performed during gene scanning where the data are typically plotted as difference curves to better magnify the differences between the melting profiles of different samples (**Figure 2D**) (Reed, et al., 2007). Conventionally, gene scanning compares unknown samples to a "normal" sequence. Overall, HRM is being used to detect small nucleotide changes, especially for single nucleotide polymorphism (SNP).

There are two major applications of high resolution melting: targeted genotyping and gene scanning. Liew et al. (2007) describes two common methods for genotyping single nucleotide polymorphisms (SNPs): unlabeled oligonucleotides (probes) and amplicon melting. Unlabeled probes are designed to detect the mutation of interest without the added cost of being fluorescently tagged (Liew, et al., 2007). This method is similar to the conventional hybridization probes except that only one probe is needed and a saturating DNA dye, LC Green I (Idaho Technologies), is used instead of covalently attached fluorescent labels (Liew, et al., 2007). Unlabeled probe assays utilize an asymmetric PCR in which one PCR primer is added in excess of the other PCR primer. As a result, two melting peaks are produced: the melting of the double-stranded amplicon and the melting of the probe off of the single-stranded product derived

from asymmetric PCR (Dames, et al., 2007). Genotyping depends on the differences in the probe melting temperatures (T_ms) (Liew, et al., 2007). In contrast to amplicon melting, there is an added cost of an additional oligonucleotide for the intended PCR reaction.

A second method for genotyping SNPs is direct amplicon melting. Direct amplicon melting was initially developed for small amplicons (<50 bp) (Liew, et al., 2004). Shorter products allows for greater differentiation because T_m differences among genotypes increases as the size of the amplicon decreases (Liew, et al., 2004). This is especially advantageous in the detection of homozygous mutations because some homozygous SNPs have melting curves identical to that of the wild-type (Palais, et al., 2005). This method does not require probes for mutation detection. Only the two primers required for PCR are needed. Genotyping is accomplished by observed changes in the shape of the melting curves or detecting a difference in T_m. Heterozygotes are easily detected by shape changes using this method, but differentiating between two homozygotes can be difficult because some base changes do not confer large differences in T_m (Liew, et al., 2007). Homozygous genotypes of class 3 and class 4 single base variants, or "base pair neutral" variants, are difficult to distinguish by simple amplicon melting (Erali, et al., 2010). They comprise approximately 12% of human single base variants and have T_m differences around 0.25°C, whereas class 1 and class 2 homozygous variants have T_m differences around 1°C (Erali, et al., 2010). Palais et al. (2005) proposed a method to better enhance homozygote detection by mixing unknown samples with samples of a known genotype. This quantitative heteroduplex analytical approach differentiates between heterozygotes, homozygotes and wild-type DNA samples. If heteroduplexes are detected, then the samples mixed are of different genotype (Palais, et al., 2005).

Another application for HRM is gene scanning. Gene scanning is the search of unknown variations in PCR amplicons prior to sequencing (HRM, 2007). This detection method uses larger sequences in detection and thus is better at detecting differences related to the presence of heteroduplexes that distort the shape of the melting curve (Reed, et al., 2007). This change in shape is best observed when comparing the normalized melting curves of a homozygous standard to a heterozygous sample (Reed, et al., 2007). If one is looking for a mutation as a result of a single base change, the difference in temperature is small, so it is magnified by plotting the data as a difference curve (**Figure 2D**). Scanning is not ideal for identifying homozygous variants within a gene. As mentioned in the previous paragraph, homozygous detection can be enhanced by adding a known reference sample to samples with unknown genotypes (Palais, et al., 2005). If the known sample is wild-type, it will form a heteroduplex when added to homozygote samples. This newly formed heteroduplex will distort the shape of the melting curve, thereby identifying the presence of a homozygous mutation. Currently, many *ACADVL* SNPs are detected by conventional sequencing methods. In order to cover an entire gene sequence using the Sanger method, many reactions are performed, and then the data from these reactions must be edited together. Depending on the gene, this process could take days or weeks to complete. Wittwer et al. (2010) proposed the use of scanning as a screening method to identify mutations in large gene regions. Confirmation of such a mutation would be far less labor intensive and align with a conventional newborn hospital stay.

Olsen et al. (2010) developed a method for HRM analysis of the *ACADVL* gene using DNA extracted from newborn screening dried bloodspots. The samples were amplified on a Peltier Thermal Cycler (Bio-Rad Laboratories), and HRM was performed on the LightScanner

(Idaho Technologies). They tested the sensitivity and specificity of the assay by performing a

blinded study with 183 samples from healthy controls and 146 samples from clinically affected

VLCADD patients. All samples were correctly genotyped using HRM analysis. A similar

method is proposed for the assay design described in this thesis; however our study utilizes

multiple PCR chemistries in which I introduce a PCR protocol that is seven times faster than

what was previously demonstrated by Olsen et al. (2010). I developed an assay that is a faster

diagnostic approach for the detection of mutations in the *ACADVL* gene using high resolution

melting analysis.
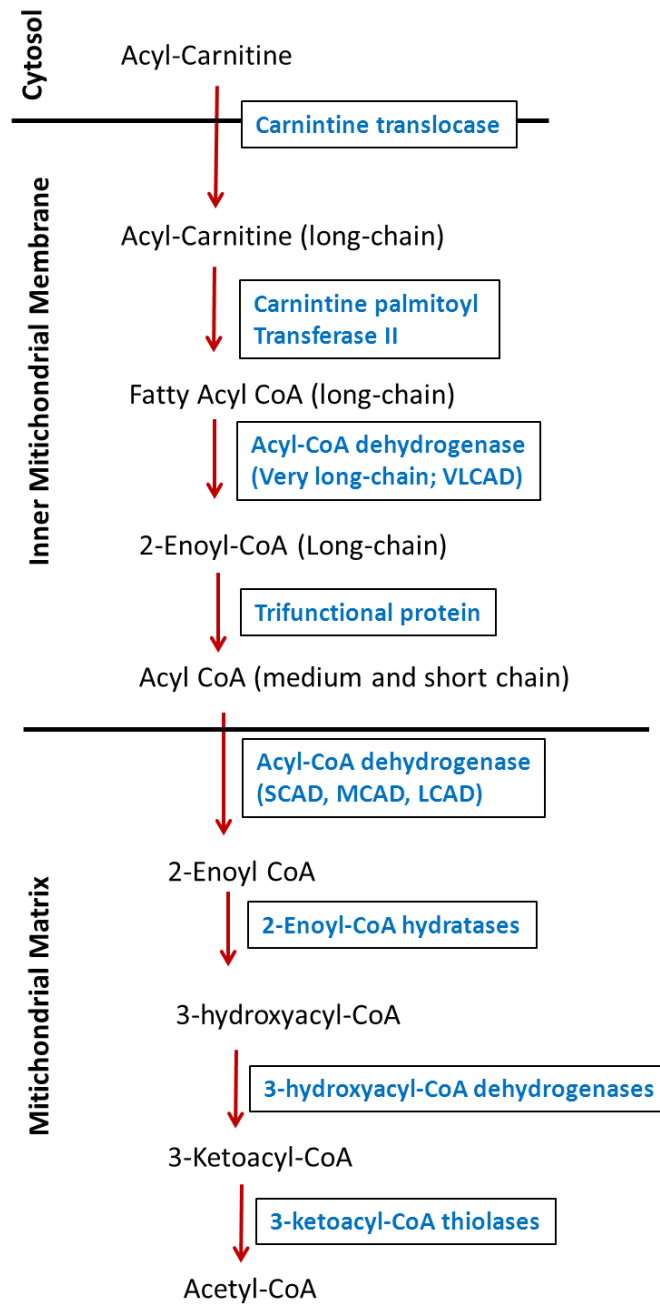
Figure 1. Fatty acid transport and beta-oxidation pathway.
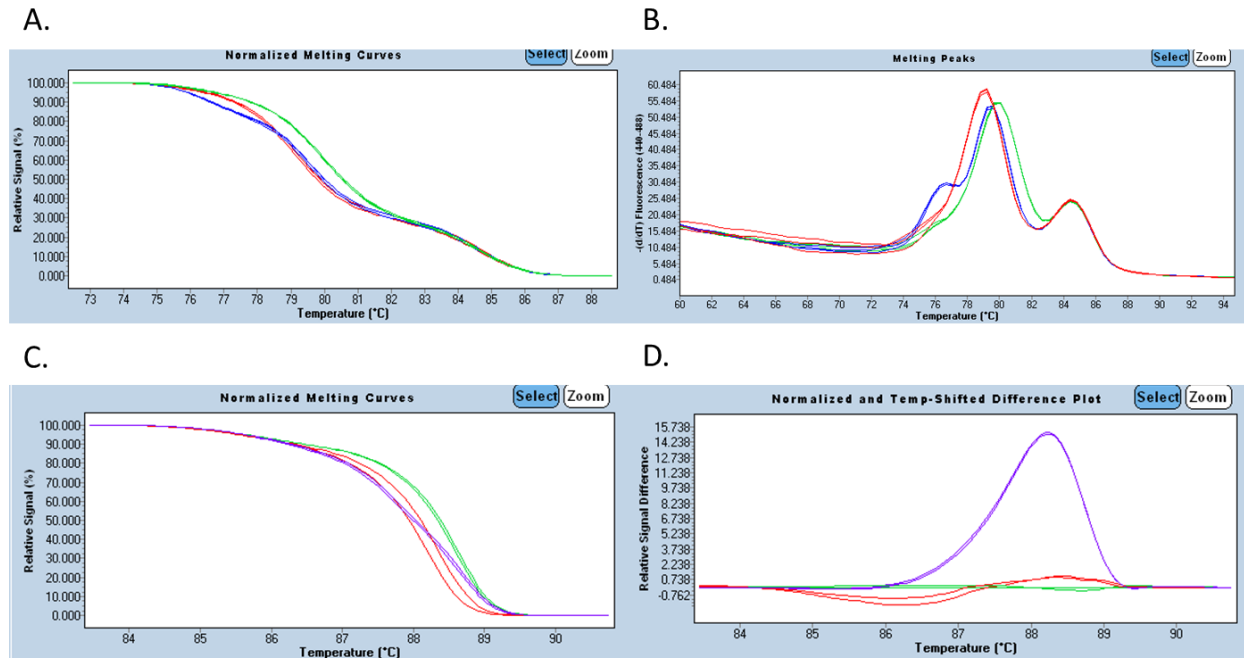
Figure 2. Two main applications of high resolution melting are genotyping and gene scanning. The genotyping results are depicted by the normalized melting curve (A) and derivative plot (B). Heterozygous (blue) and homozygous (red) mutants are distinguishable from the wild-type (green). The gene scanning results are depicted by the normalized melting curve (C) and difference plot (D). Heterozygous (purple) and homozygous (red) mutants are distinguishable from the wild-type (green).

CHAPTER II

MATERIALS AND METHODS

Primer Design

The primer design was performed by a senior scientist on the Research and Development team at Canon US Life Sciences, Inc. This section is in reference to the following technical report: *ACADVL Scanning Feasibility on the Light Cycler 480* (Benkhadra, Papazisi, & Huuskonen, 2013). The primer pairs were positioned on the intronic regions of the gene, so each PCR product (amplicon) corresponded to an entire exon.

VisualOMP^{TM} software package (DNA Software Inc.) was used for primer design using ACADVL reference sequence with NCBI accession number NG_007975. For the two-step PCR conditions aiming at an annealing and extension temperature of 70°C, primer pairs were designed and selected based on the follow main criteria (Benkhadra, Papazisi, & Huuskonen, 2013):

- PCR chemistry: 50 mM NaCl, 2.96 mM MgCl$_2$, 2% DMSO, 1M Betaine, and pH=7.0 (pH is the only fixed condition in the VisualOMP^{TM} software package).

- Binding kinetics and melting temperature (T$_m$) of the primers.

- The distance between the forward primer's 3' end and exon's 5' end (sense strand), as well as distance between the forward primer's 3' end and exon's complementary sequence 5' (anti-sense strand) were preferred to be ≥15 bp and ≤5 bp respectively.

- Amplicon length was preferred not to exceed ≤ 300 bp.

- Primers with minimal binding capacity between ≥ 90% and <100% were accepted; however those with binding capacity between ≥95 and <100% were preferred.

- Primer pairs with ΔG ≤-2kcal were accepted, but not preferred.

Non-specific primer binding was investigated using the ThermoBlast[TM] software package (DNA Software Inc.) and PrimerBlast[3], NCBI's online tool. Primer pairs that showed non-specific binding were omitted ($-4 < \Delta G < -2$) (SantaLucia Jr., 2007).

PCR Efficiency

Each set of primers was screened on the Light Cycler 480 (Roche Diagnostics, Indianapolis, IN) and the BioRad CFX (Bio-Rad, Hercules, CA). During the time period when this study was conducted, a major effort was carried out simultaneously to optimize the PCR chemistry to ultimately suit the prototype instrument that was being developed at CLS. Hence, three different PCR chemistries were used in this set of experiments: Takara Ex Taq Hot Start Polymerase (Clontech, Mountain View, CA) with 10X Canon US Life Sciences (CULS) buffer, Titanium Klentaq DNA Polymerase (Clontech) with 2X CULS buffer pH 8.5, and Titanium Klentaq DNA polymerase with AT Buffer. Each time the chemistry was changed, the experiments were repeated to ensure that PCR efficiency was not affected.

The first two chemistries listed (10X CULS buffer and 2X CULS buffer pH 8.5) were used in the initial primer screening experiments. Multiple primer pairs were designed for each assay, and this set of experiments established the best primer pair for each exon. Genomic DNA from cell line NA11254 and from NA09820 (Coriell Cell Repository, Camden, NJ) was used as the template. All PCR reaction mixtures contained 3 mM $MgCl_2$, 0.2% BSA, 1.6 mM dNTPs, 1 μm of each primer and 1X LC Green Plus[TM] (Idaho Technologies, Salt Lake City, UT) and 10 ng/μl of DNA in a final reaction volume of 10 μL. The 10X CULS buffer did not contain 1M Betaine or 2% DMSO, so these constituents were added separately to the master mix.

---

[3] Primer Blast: http://www.ncbi.nlm.nih.gov/tools/primer-blast/

The PCR chemistry was changed from the CULS buffer system to the AT buffer system. The primer pairs selected for each assay were retested on the Light Cycler 480 in the AT Buffer. This is a three component system consisting of a DNA Dilution Buffer, Primer Master Mix, and DNA Master Mix. All PCR reaction mixtures contained 20 mM Tris-HCl pH 8.3, 30 mM KCl, 1M Betaine, 2% DMSO, 0.05% BSA, 4.5 mM $MgCl_2$, 0.04% Tween20, 1X Titanium Taq Polymerase (Clontech, Mountain View, CA), 1 µM primers, 9 ng/µl of genomic DNA (cell line NA11254), 1.5 mM dNTPs, and 1X LC Green Plus[TM] (Idaho Technologies, Salt Lake City, UT). The components were added in a 1:1:1 ratio in a final PCR reaction volume of 18 µl.

The performance of the primers was dependent on the PCR cycling conditions as well as the buffer system that was used. After the change to the AT Buffer system, re-optimization of the PCR cycling conditions was required for most of the assays. **Table 1** lists the cycling conditions selected in CULS buffer as well as the new conditions established with the AT buffer system.

The amplification plots shown in **Figure 3** represent three different scenarios: ideal amplification plot with the curves reaching plateau; acceptable amplification plot with high maximum fluorescence (relative fluorescence units or RFUs) levels; and very poor amplification with high crossing point (Cp) values and low fluorescence levels. These three scenarios were common during the cycling optimization process on the LightCycler 480. Primers for each assay were scored based on specific amplification criteria as well as the purity of the PCR product. Crossing point (Cp) values above 28 cycles were considered poor, and signal-to-noise (SNR) ratios greater than 2.5 were optimal.

The Caliper LabChip GX (Perkin Elmer, Waltham, MA) is a genetic analyzer that performs electrophoretic separation of samples on a microfluidic platform. It provides

information such as PCR product (amplicon) size, amplicon purity, and sample concentration. In this set of experiments, the purity of the target for chosen assays was greater than 95% (**Appendix Figure 4**). After carefully evaluating the data, the best performing pairs were chosen for genotyping.

Genotyping with Synthetic Constructs

Genomic DNA samples containing known mutations for the *ACADVL* were not readily available. One method to evaluate the feasibility of an assay is by designing synthetic constructs containing specifically selected mutations. The constructs behave similarly to genomic DNA in terms of PCR and melting properties. In this study, we designed a series of synthetic constructs for all 20 exons of the *ACADVL* (Gene Oracle, Mountain View, CA). The constructs were designed to contain two neighboring exons per construct, with an intervening intronic sequence (~200 bp) in between. This helped reduce the total number of constructs and processing steps. Upon receipt from Gene Oracle, the constructs were diluted 1:10 in TE buffer pH 7.0 (1 µl construct in 9 µl TE buffer) (Ambion, Grand Island, NY). The concentration of each construct was measured in triplicate on the Nanodrop 2000 (Thermo Fisher Scientific, Rockville, MD), averaged and recorded. The constructs were further diluted to the following working concentrations: 100 pg/µl, 5 pg/µl and 0.067 pg/µl. A list of the *ACADVL* synthetic constructs can be found in **Table 2**.

The following experiments were performed for exons 1, 3-17, 19 and 20. Wild-type (pWT), homozygote (pHM), and heterozygote (pHT) construct DNA were used to genotype on the Light Cycler 480. Heterozygotic construct was made by mixing equal quantities of the wild-type and homozygote plasmid DNA (pDNA) together. Genomic DNA extracted from cell line

NA11254 and NA09820 (Coriell Cell Repositories, Camden, NJ) were used to examine initial

performance with the genomic DNA. The final template concentration of 5 copies/nl was

matched for genomic DNA and construct DNA in the 10 µl reaction mixture on the Light Cycler

480.

The PCR chemistry used was 1X Titanium Klentaq DNA polymerase (Clontech,

Mountain View, CA) with 2X CULS buffer pH 8.5. All PCR reaction mixtures contained 3mM

$MgCl_2$, 0.2% BSA, 1.6 mM dNTPs, 1 µm of each primer, 1X LC Green Plus^{TM} (Idaho

Technologies, Salt Lake City, UT) in a final reaction volume of 10 µL. PCR was performed with

a 2-minute hot-start at 95°C. The cycling conditions, however, varied with each assay. The

results were analyzed on the Light Cycler 480 Gene Scanning software. Similar to the PCR

efficiency tests, the best cycling conditions were chosen based on Cp values, signal-to-noise ratio

(SNR), and amplification curve fluorescence level.

The PCR chemistry used in the genotyping experiment for exon 2 was Titanium Klentaq

DNA polymerase with AT Buffer. Wild-type, homozygote, and heterozygote construct DNA

were used to genotype on the Light Cycler 480 (Roche Diagnostics). Heterozygotic construct

was made by mixing equal quantities of the wild-type and homozygote DNA together. The PCR

reaction mixtures contained 20 mM Tris-HCl pH 8.3, 30 mM KCl, 1M betaine, 2% DMSO,

0.05% BSA, 4.5 mM MgCl2, 0.04% Tween20, 1X Titanium Taq Polymerase, 1 uM primers, 9

ng/µl of genomic DNA (cell line NA11254) or 0.4 pg/µl of plasmid DNA, 1.5 mM dNTPs, and

1X LC Green Plus^{TM} (Idaho Technologies). The final PCR reaction volume was 18 µl. The

results were analyzed on the Light Cycler 480 Gene Scanning software.

Blinded Study using Genomic DNA

In this study, a sample of 30 randomly selected genomic DNAs readily available in the laboratory were chosen. **Table 3** lists the cell lines and the corresponding number used to identify each DNA sample. The genotypes of these samples were unknown for the *ACADVL* gene. Each exon was tested with the 30 samples, and wild-type, homozygote, and heterozygote synthetic constructs were used as controls. The 3-component AT buffer system was used in this set of experiments. All PCR reaction mixtures contained 20 mM Tris-HCl pH 8.3, 30 mM KCl, 1M Betaine, 2% DMSO, 0.05% BSA, 4.5 mM $MgCl_2$, 0.04% Tween20, 1X Titanium Taq Polymerase, 1 uM primers, 9 ng/µl of genomic DNA or 0.4 pg/µl of plasmid DNA, 1.5 mM dNTPs, and 1X LC Green Plus[TM] (Idaho Technologies, Salt Lake City, UT). The final PCR reaction volume was 18 µl. The genomic DNA samples as well as the synthetic constructs were run in duplicate on a 96-well plate array, and PCR and HRM were carried out on the Light Cycler 480. The HRM data was analyzed with the Light Cycler 480 Gene Scanning software package.

Sequencing Protocol

The samples selected for sequencing were chosen based on the difference in their melting pattern compared to the melting pattern of the wild-type plasmid DNA. Once selected, the concentrations of each were determined by running the samples on the Caliper Lab Chip GX genetic analyzer (Perkin Elmer, Waltham, MA). The final reaction volume required by the Caliper GX for a 96 well plate set-up is 40 µl. In order to achieve this volume, 10 µl of sample was added to 30 µl of nuclease-free water (Ambion) and plated on a BioRad hard-shell 96 well plate array. The concentrations ranged from 9 ng/µl-120 ng/µl, which was equal to or greater

than the recommended concentration for sequencing (5 ng/µl-20 ng/µl). The PCR primers, both

forward and reverse, were diluted in nuclease-free water to 5 µM. Macrogen (Rockville, MD)

performed the sample purification and sequencing experiments. The results were analyzed with

CodonCode Aligner software version 3.7.1 (CodonCode Corporation, Centerville, MA).

Exon	CULS Buffer PCR Conditions	AT Buffer PCR Conditions
1	98C/3s-70C/15s x40c	98C/3s-72C/12s x40c
2	98C/3s-70C/12s x40c	98C/3s-76C/15s x40c
3	98C/3s-68C/15s x40c	98C/3s-68C/12s x40c
4	98C/3s-70C/15s x40c	98C/3s-70C/12s x40c
5	98C/3s-70C/7s x40c	98C/3s-72C/12s x40c
6	98C/3s-70C/15s x40c	98C/3s-70C/12s x40c
7	98C/3s-68C/12s x40c	98C/3s-70C/12s x40c
8	98C/3s-68C/12s x35c	98C/3s-70C/12s x40c
9	98C/3s-68C/20s x40c	98C/3s-72C/12s x40c
10	98C/3s-68C/20s x40c	98C/3s-72C/12s x40c
11	95C/3s-68C/12s x40c	98C/3s-68C/12s x35c
12	98C/3s-68C/12s x35c	98C/3s-68C/12s x35c
13	98C/3s-70C/7s x40c	98C/3s-70C/12s x35c
14	98C/3s-68C/15s x40c	98C/3s-68C/12s x40c
15	98C/3s-68C/12s x35c	98C/3s-72C/12s x35c
16	98C/3s-68C/12s x35c	98C/3s-72C/12s x35c
17	98C/3s-68C/12s x35c	98C/3s-72C/12s x40c
19	98C/3s-68C/12s x35c	98C/3s-68C/12s x40c
20	98C/3s-68C/12s x35c	98C/3s-68C/12s x40c

Table 1. A comparison between the optimal PCR cycling conditions selected in the CULS

buffer and the conditions selected when the primers were screened in the AT buffer.

A.

B.

C.
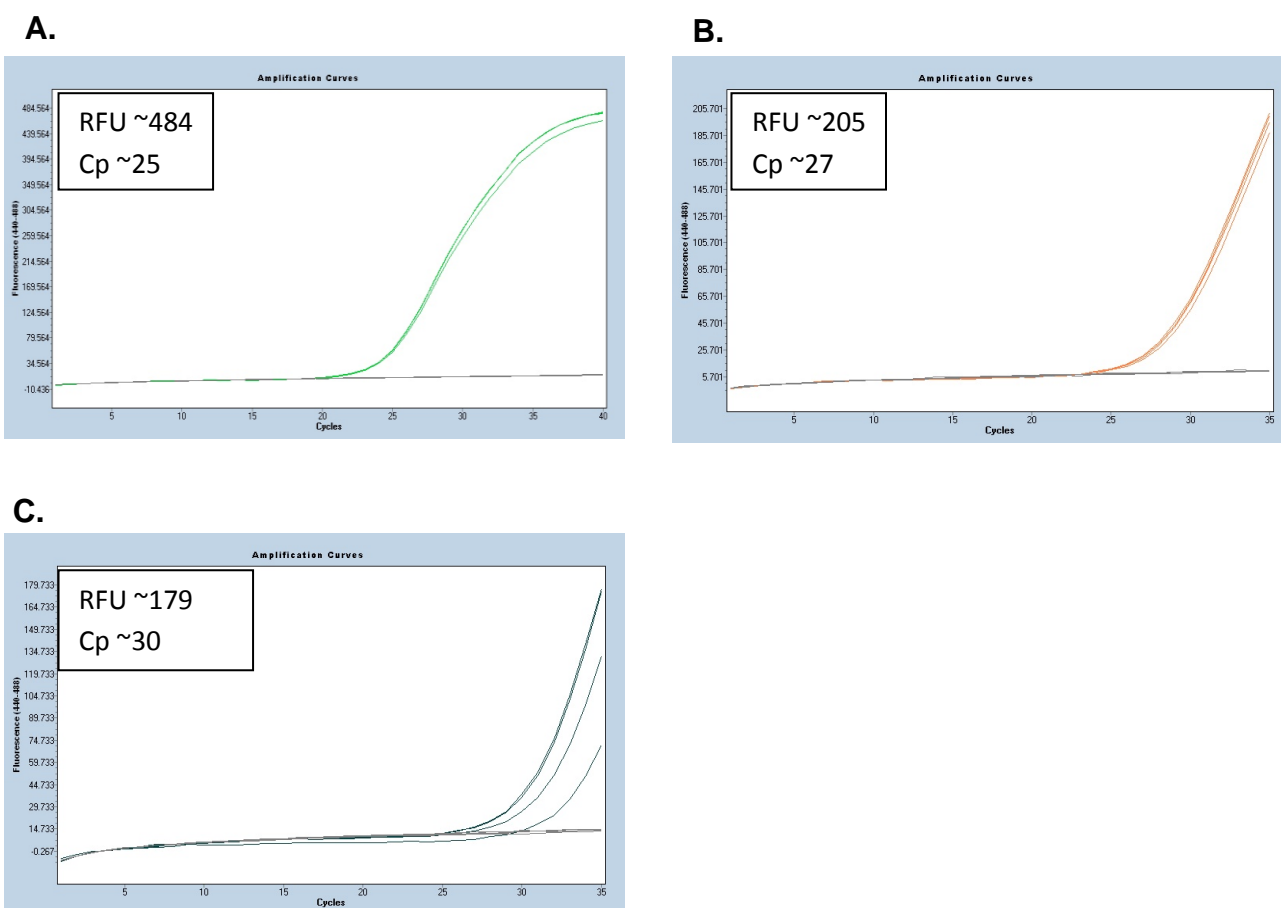
Figure 3. **Three examples of PCR cycling optimization on the Light Cycler 480 using**

genomic DNA as template. The first example (**A**) represents ideal cycling conditions where the

PCR reaches a plateau. The second example (**B**) represents acceptable cycling conditions where

the curves do not quite reach plateau, but achieve a high maximum fluorescence. The third

example (**C**) represents poor PCR performance (high Cp and low maximum RFU) and requires

further optimization using different conditions.

Target Exon	Synthetic Construct Name	Length in bp	Genotype	Mutation
1&2	ACADVL_x01x02_WT	464	WT	
3&4	ACADVL_x03x04_WT	402	WT	
5&6	ACADVL_x05x06_WT	482	WT	
7&8	ACADVL_x07x08_WT	670	WT	
9&10	ACADVL_x09x10_WT	720	WT	
1&2	ACADVL_x01x02_61p1GA_65CA	464	HOM	c.62+1G>A; c.65C>A
3&4	ACADVL_x03x04_194CT_227GA	402	HOM	c.194C>T; c.227G>A
5&6	ACADVL_x05x06_339CA_364AG	482	HOM	c.339C>A; c.364A>G
7&8	ACADVL_x07x08_553GA_623m2AC	670	HOM	c.553G>A; c.623-2A>C
9&10	ACADVL_x09x10_779CT_897GT	720	HOM	c.779C>T; c.897G>T
11&12	ACADVL_x11x12_WT	565	WT	
13&14	ACADVL_x13x14_WT	429	WT	
15&16	ACADVL_x15x16_WT	426	WT	
17&18	ACADVL_x17x18_WT	431	WT	
19&20	ACADVL_x19x20_WT	585	WT	
11&12	ACADVL_X11X12_1096CT_1213GC	565	HOM	1096C>T; 1213G.C
13&14	ACADVL_x13x14_1322GA_1349GA	429	HOM	1322G>A; 1349G>A
15&16	ACADVL_x15x16_1505TC_1600GA	426	HOM	1505T>C; 1600G>A
17&18	ACADVL_x17x18_1621del1_1714GA	430	HOM	1621del1; 1714G>A
19&20	ACADVL_x19x20_1824CT_1837CT	585	HOM	1824C>T; 1837C>T

Table 2. ACADVL scanning assay synthetic construct designs. Each construct was designed to contain two neighboring exons.

CLS #	1	2	3	4	6	11	15	16	19	22
Cell Line	NA01531	NA07441	NA07552	NA08338	NA11277	NA11284	NA11859	NA11860	NA12785	NA18799
CLS #	23	50	51	65	71	73	79	85	316	317
Cell Line	NA18800	NA11254	NA11255	NA09820	NA13033	NA21551	NA02828	NA18803	NA14712	NA14899
CLS #	318	319	320	391	392	395	396	490	495	499
Cell Line	NA16000	NA20730	NA16028	NA07523	NA08684	NA14448	NA14501	HeLa Cells	NA17247	NA17130

Table 3. A list of the 30 different DNA samples selected for the blinded study. Each cell line was assigned a number (CLS #) upon receipt. The cell lines were purchased from Coriell Cell Repositories (Camden, NJ), and the expansion and extraction of the DNA were performed by Texcell (Frederick, MD).

CHAPTER III

RESULTS

PCR Efficiency

Three different PCR chemistries were used in this study; however, the initial primer

screening experiments were performed in the following buffer systems: Takara Ex Taq Hot Start

Polymerase (Clontech) with 10X CULS buffer and Titanium Klentaq DNA Polymerase

(Clontech) with 2X CULS buffer pH 8.5. Once these experiments were complete, the primers

were evaluated based on the following criteria: PCR Cp value, RFU of the amplification curve,

and Caliper GX data. Samples below 95% purity were not selected for genotyping. Generally,

no-template control (NTC) amplification was associated with the lower purity of the product,

indicating the possibility of non-specific product and/or primer-dimer formation. **Table 4**

contains a summary of the original amplification data for each primer pair selected for

genotyping experiments on the Light Cycler 480.

When the PCR chemistry was changed, the primers were reevaluated in the AT buffer

with Titanium Klentaq DNA polymerase on the Light Cycler 480. Different primer pairs for

exon 6 and exon 13 were used: 224/177 and 559/560, respectively. Each yielded a more efficient

PCR and purer product compared to the previous primer pairs used for exon 6 and exon 13. The

previously established cycling conditions required optimization in the AT buffer system. For

most of the assays, the annealing temperature and/or cycling times were changed. The new

conditions were chosen based on the following criteria: Cp values, maximum fluorescence of the

amplification curve, and Caliper GX data. **Table 5** contains a summary of the amplification

results for each primer pair. The design characteristics for each primer pair that was chosen for

genotyping are listed in **Table 6**.

Genotyping with Synthetic Constructs

       Table 7 summarizes data from the PCR experiments using construct DNA in the CULS

buffer. The PCR efficiency was evaluated based on the following criteria: Cp values, SNR,

Caliper GX data, and gene scanning results. The Caliper GX provided the purity of the sample

(wild-type target amplicons were >96% pure) and size of the target **(Appendix Figure 5).** The

purity of the heterozygous samples was <95% for some of the assays tested. In these instances,

there was a secondary product present that was similar in size to the target amplicon. An

example from exon 17 is shown in **Appendix Figure 6**. The Light Cycler 480 gene scanning

software was used to analyze the genotyping results from this set of experiments. Based on the

results derived from the Light Cycler 480 melting analysis software, all construct heterozygotes

were detectable. Homozygote variants were detectable in 12 out of 19 assays as well (Exons 1, 2,

5, 6, 8, 11, 12, 13, 15, 17, 19, and 20). **Table 8** is a summary of the genotyping results from this

set of experiments.

Blinded study using genomic DNA

In the experiments performed with the 30 different genomic DNA samples, a true wild-type genomic DNA was not known for the *ACADVL*. The data were analyzed with the Roche LightCycler 480 Gene Scanning software package. Wild-type plasmid DNA was selected as the baseline for the analysis. Samples with a relative fluorescence difference of +/- 1.0 or greater from the normalized baseline (plasmid wild-type) were selected as candidates for sequencing. Samples within +/- 1.0 units from the baseline were also selected for sequencing. This was a very conservative selection since we had no prior experience on what magnitude of difference to expect from potential heterozygous samples. In a real clinical setting, the cut-off value would have been predetermined by using known samples with mutations, as well as to determine the sensitivity and specificity of a particular assay.

The difference plot for exon 16 is depicted in **Figure 7**. There are five distinct melting patterns. Samples from each group were selected for sequencing. The same selection criteria were used for the other assays (**Appendix Figures 8-25**). After careful analysis of each assays' melting curves, 85 samples were chosen for sequencing. **Table 9** contains a list of all DNA samples sent for sequencing and the confirmed genotypes.

Sequencing Results

A total of 85 samples were sequenced bi-directionally by Macrogen (Rockville, MD) using automated Sanger sequencing technology. Upon receipt of the sequencing results, the files were uploaded into sequence alignment software, Codon Code Aligner. The amplicon sequences were downloaded from NCBI BLAST and uploaded into Codon Code Aligner as well. The software is capable of aligning the forward and reverse strands to the amplicon reference sequence. If a mutation is present, the nucleotide is not defined. It is typically given an arbitrary "N" value.

A total of 21 of the 85 samples sent for sequencing contained a mutation. From the 21 mutated samples, 7 different mutations were identified with the Codon Code Aligner software. The location and frequency of each mutation are listed in **Table 10**. Alamut, a sequence alignment and annotation software, was used to identify the types of mutations that were found and where they were located on the gene. Alamut confirmed that each mutation discovered was a single nucleotide polymorphism (SNP). The frequency of each mutation in nature, as reported by NCBI's dbSNP database, was very similar to the frequency calculated in this study with a sample size of 30 **(Table 10)**. The low number of mutations detected in these samples is aligned with our prediction that the low cut-off value in a difference plot (see description above) would result in most samples showing no mutations.

LC 480 Data					
Target	Primer Pair	Cycling Conditions	SNR	Cp Values	PCR Cycles
Exon 01	x01_88/336m	98C/3s-68C/12s	5.42	24.67	40.00
Exon 03	x03_134/115	98C/3s-68C/12s	7.50	24.51	40.00
Exon 04	x04_175/196	98C/3s-68C/12s	7.74	24.85	40.00
Exon 05	x05 257/258	98C/3s-70C/12s	5.54	25.88	40.00
Exon 06	x06_4/79	98C/3s-70C/15s	8.81	25.09	40.00
Exon 07	x07 3352/328	95C/3s-68C/12s	5.19	26.61	35.00
Exon 08	x08_206/253	98C/3s-70C/15s	6.82	26.18	40.00
Exon 09	x09_153/160	98C/3s-68C/20s	7.37	23.54	40.00
Exon 10	x10 355/360	98C/3s-68C/20s	8.73	23.92	40.00
Exon 11	x11 311/314	95C/3s-68C/12s	5.36	26.50	35.00
Exon 12	x12 233/236	95C/4s-70C/6s	4.87	28.02	35.00
Exon 13	x13_551/562	98C/3s-68C/12s	6.74	24.69	40.00
Exon 14	x14_72/73	98C/3s-68C/12s	6.85	29.20	40.00
Exon 15	x15_125/126	98C/3s-68C/12s	7.18	26.28	40.00
Exon 16	x16_15/16	98C/3s-68C/12s	5.25	26.87	40.00
Exon 17	x17_51/52	98C/3s-68C/12s	4.82	24.31	40.00
Exon 19	x19_48/49	98C/3s-68C/12s	5.93	24.92	40.00
Exon 20	x20_13/14	98C/3s-68C/12s	4.62	29.52	40.00

Table 4. The ampification data for each primer pair selected during the PCR efficiency experiments in the CULS buffer system.

Exon	Primer Pair	Cycling Conditions	CP	SNR
1	x01_88/336m	98C/3s-72C/12s x40c	24.67	9.75
2	x02_7m4/8	98C/3s-76C/15s x40c	27.01	8.61
3	x03_134/115	98C/3s-68C/12s x40c	24.61	10.88
4	x04_175/196	98C/3s-70C/12s x40c	23.78	8.15
5	x05_257/258	98C/3s-72C/12s x40c	24.73	9.66
6	x06_224/177	98C/3s-70C/12s x40c	24.65	14.22
7	x7_3352/328	98C/3s-70C/12s x40c	24.91	13.84
8	x8_206/253	98C/3s-70C/12s x40c	24.84	11.80
9	x09_153/160	98C/3s-72C/12s x40c	24.85	14.61
10	x10_355/360	98C/3s-72C/12s x40c	24.82	16.98
11	x11_311/314	98C/3s-68C/12s x35c	23.58	7.07
12	x12_233/236	98C/3s-68C/12s x35c	23.30	8.51
13	x13_559/560	98C/3s-70C/12s x35c	24.77	10.30
14	x14_72/73	98C/3s-68C/12s x40c	25.18	9.69
15	x15_125/126	98C/3s-72C/12s x35c	25.23	15.13
16	x16_15/16	98C/3s-72C/12s x35c	25.04	12.20
17	x17_51/52	98C/3s-72C/12s x40c	25.07	9.94
19	x19_48/49	98C/3s-68C/12s x40c	23.30	7.63
20	x20_13/14	98C/3s-68C/12s x40c	23.53	6.97

Table 5. The ampification data for each primer pair selected during the PCR efficiency experiments in the AT buffer system.

ACADVL Exon Target Assays	Primer Pair	Amplicon Size	Amplicon GC%	Primer Names	Sequence	Length	GC%	Tm
1	x01_88/336m	160	71%	Vx01_88	GACGCCAGAGCTGGGTCAGAGC	22	68%	73.0
				Vx01_336m	GTGCCCAGGGCCGCTGCCCAC	21	81%	77.0
2	x02_7m4/8	178	77%	Vx02_7m4	CGAAGCGGACCGCCGCTCCCACA	23	74%	73.0
				Vx02_8	TGGGCAGCGGCCCTGGGC	18	89%	77.0
3	x03_134/115	168	58%	Vx03_134	GTTCTCCCCTTGACACAGCGGAAGTC	26	58%	75.3
				Vx03_115	TTGGGTCTGGCTAAGGTCCACCTGGC	26	62%	77.5
4	x04_175/196	156	55%	Vx04_175	CCTGGCCCCACCCAGCTCTGATTA	24	63%	75.6
				Vx04_196	TAGCCAGACCCAACCAGAGCCCTG	24	63%	75.6
5	x05_257/258	173	59%	x05_257	ACATCTCCAAACACCTCACCAGGGACC	27	56%	76.7
				x05_258	GGGCCAGGGTGGTTTCCCCTGCCA	24	71%	77.6
6	x06_224/177	252	60%	x06_224	CCCTGGTGAGGTGTTTGGAGATGTTAAG	28	50%	75.1
				x06_177	CCAAGCTGGGGTATGGCATACTGGGA	26	58%	76.1
7	x7_3352/328	249	59%	Vx07_3352	CCTAATCTGTGCCAAGCCCAGTGTGC	26	58%	75.7
				Vx07_328	CCCCTGCAGCCAGTGACAACCCCA	24	67%	76.6
8	x8_206/253	247	57%	Vx08_206	GGAAGTGGGCCGAGGGGACTTTGA	24	63%	75.2
				Vx08_253	TGGGGCCTGGAATTGGGCGGAG	22	68%	76.1
9	x09_153/160	243	58%	Vx09_153	TCTGCCCAGGAGCCCAGTCCTGCC	24	71%	79.3
				Vx09_160	TTCCAGGCCCCACTGCTCCCCGTC	24	71%	77.5
10	x10_355/360	308	56%	Vx10_355	GGGGACAGTGAGACTTCTGTTTGGGTTACCTAG	33	52%	77.1
				Vx10_360	CCCCAGTGACAACCTGTTGAACACAC	26	54%	74.0
11	x11_311/314	212	55%	Vx11_311	GGAAGAAAGCCCCAGGGCTCCAGGGAGA	28	64%	78.9
				Vx11_314	TCCTAGGGAGACTGCAGAACCACACTGAA	29	52%	74.0
12	x12_233/236	209	54%	Vx12_233	GAGACTGGTTTTGGGAGCTGAGCACC	26	58%	75.6
				Vx12_236	CCAAGTCTGACAAAGCCCTTTGCAATT	27	44%	74.1
13	x13_559/560	138	54%	Vx13_559	GCCGAGGCTCTGCAGAAGACCGTC	24	67%	76.6
				Vx13_560	GGTGCTCAGCTCCCAAAACCAGTC	24	58%	73.8
14	x14_72/73	190	54%	Vx14_72	GGCACATCTCAGCACGGGCATATAA	25	52%	70.3
				Vx14_73	ACTGTCCTCCCCACCTCTACCCC	23	65%	70.4
15	x15_125/126	183	59%	Vx15_125	TGCCATACACCACCCTGCCCTCC	23	65%	71.3
				Vx15_126	GACAGTGAGTCCTGACTGCTGG	22	59%	69.4
16	x16_15/16	157	63%	Vx16_15	CTGATGCAGGCTCTCCTGGACC	22	64%	70.0
				Vx16_16	GCAGGGTGGTGTATGGCAACTAACC	25	56%	70.1
17	x17_51/52	153	57%	Vx17_51	AGGAGAGGAAAGGGAGGGGCGG	22	68%	70.9
				Vx17_52	GGCCCCTCTGAGCCCCGCACT	21	76%	72.8
19	x19_48/49	155	59%	Vx19_48	CCTCACCTGAGCTTGGCAGCCC	22	68%	70.1
				Vx19_49	GGATCCCAGCCGGCCCAGATTTAT	24	58%	69.4
20	x20_13/14	249	63%	Vx20_13	TTCGGCTTTGGCTTGAGGGAAGG	23	57%	68.3
				Vx20_14	GCTCAGGTGAGGGCTGGAGGTGCA	24	67%	71.6

Table 6. Primer Pair design characteristics for each of the ACADVL scanning assays.

ACADVL Exon	Primer Pair	Number of HRM Domains	Construct	PCR conditions (Cycle #)	SNR	Cp Values
1	x01_88/336m	1	WT	two step 98C-70C 3s-15s [40x]	6.84	28.72
2*	7m4/8	1	WT	two step 98C-76C 3s-15s [40x]	11.49	26.64
3	x03_134/115	1	WT	two step 98C-68C 3s-15s [40x]	9.15	28.60
4	x04_175/196	1	WT	two step 98C-70C 3s-15s [40x]	9.31	29.15
5	x05_257/258	1	WT	two step 98C-70C 3s-7s [40x]	3.88	35.00
6	x06_4/79	1	WT	two step 98C-70C 3s-15s [40x]	7.91	31.71
7	x7_3352/328	1	WT	two step 98C-68C 3s-12s [40x]	4.98	35.00
8	x8_206/253	1	WT	two step 98C-68C 3s-15s [35x]	4.04	30.00
9	x09_153/160	1	WT	two step 98C-68C 3s-20s [40x]	8.86	30.13
10	x10_355/360	2	WT	two step 98C-68C 3s-20s [40x]	11.03	30.86
11	x11_311/314	1	WT	two step 98C-68C 3s-12s [40x]	6.16	32.47
12	x12_233/236	2	WT	two step 98C-68C 3s-15s [40x]	6.17	30.00
13	x13_559/560	1	WT	two step 98C-70C 3s-7s [40x]	7.64	32.30
14	x14_72/73	1	WT	two step 98C-68C 3s-15s [40x]	8.02	32.61
15	x15_125/126	1	WT	two step 98C-68C 3s-12s [35x]	7.02	29.55
16	x16_15/16	2	WT	two step 98C-68C 3s-12s [35x]	6.15	29.44
17	x17_51/52	1	WT	two step 98C-68C 3s-12s [35x]	5.73	28.42
19	x19_48/49	1	WT	two step 98C-68C 3s-12s [35x]	6.26	29.62
20	x20_13/14	1	WT	two step 98C-68C 3s-15s [40x]	4.94	28.98

Table 7. The ampification data for each primer pair selected during the PCR efficiency experiments using plasmid DNA as the template. The plasmids showed a 2-3 cycle delay in amplification compared to the genomic DNA samples. This could be resolved by increasing the concentration of the pDNA to match the gDNA samples.

* Genotyping experiments for exon 2 were performed in the AT buffer because it had not been optimized during the initial tests in the CULS buffer.

Exon	Mutation	Class	HET	HOM
1	c.62+1G>A	I		
2	c.65C>A	II		
3	c.194C>T	I		
4	c.227G>A	I		
5	c.339C>A	II		
6	c.364A>G	I		
7	c.553G>A	I		
8	c.623-2A>C	II		
9	c.779C>T	I		
10	c.897G>T	II		
11	c.1096C>T	I		
12	c.1213G>C	III		
13	c.1322G>A	I		
14	c.1349G>A	I		
15	c.1505T>C	I		
16	c.1600G>A	I		
17	c.1621del1	del		
19	c.1824C>T	I		
20	c.1837C>T	I		

Table 8. ACADVL Scanning assay genotyping results from the Light Cycler 480. Exon 2 is the only assay evaluated in the AT buffer for this data set. The cells highlighted in yellow represent instances where the software clustered the construct wild-type and construct homozygote together even though the patterns generated by the difference plot were different. If there was variability among replicates, the cell was highlighted yellow. If the homozygote variant and its wild-type were indistinguishable, the cell is highlighted red. For clear genotyping results, the cell is highlighted green.
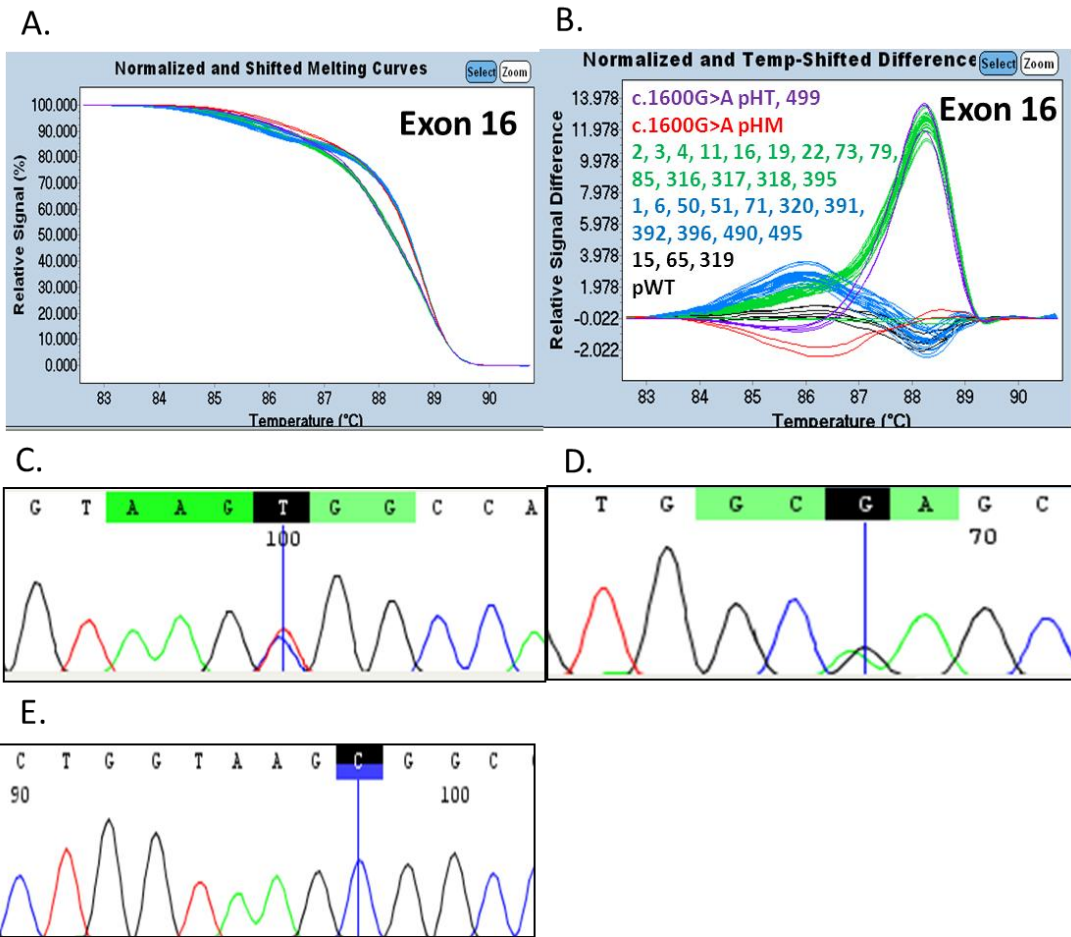
Figure 7. Summary of *ACADVL* exon 16 HRM scanning and sequencing results.

Normalized HRM curve (A), difference plot (B) and sequencing results (C-E) from Exon 16

blinded experiments with 30 randomly selected genomic DNA samples from. The difference

plot shows 5 distinct groups: blue, green, purple, red and black. The sample colors were

manually assigned. The sequencing results (C) confirmed the presence of a heterozygous

mutation: c.1605+6T>C. The sequencing results (D) confirmed the presence of a heterozygous

mutation: c.1600G>A. The sequencing results (E) confirmed the presence of a homozygous

mutation: c.1605+6T>C.

	DNA Samples								
Exon 1	DNA 2	DNA 3	DNA 395						
Exon 2	DNA 2	DNA 3	DNA 19						
Exon 3	DNA 2	DNA 3	DNA 19						
Exon 4	DNA 2	DNA 3	DNA 395						
Exon 5	DNA 2	DNA 3	DNA 11	DNA 23	DNA 395				
Exon 6	DNA 2	DNA 3	DNA 19	DNA 392					
Exon 7	DNA 2	DNA 3	DNA 19						
Exon 8	DNA 1	DNA 2	DNA 3	DNA 4	DNA 499				
Exon 9	DNA 2	DNA 3	DNA 19	DNA 11	DNA 23	DNA 499			
Exon 10	DNA 2	DNA 3	DNA 15	DNA 23					
Exon 11	DNA 2	DNA 3	DNA 79						
Exon 12	DNA 2	DNA 3							
Exon 13	DNA 2	DNA 3	DNA 19	DNA 79	DNA 392	DNA 499			
Exon 14	DNA 2	DNA 3							
Exon 15	DNA 2	DNA 3	DNA 392						
Exon 16	DNA 2	DNA 3	DNA 4	DNA 6	DNA 11	DNA 15	DNA 16	DNA 19	DNA 22
	DNA 23	DNA 73	DNA 79	DNA 85	DNA 316	DNA 317	DNA 318	DNA 395	DNA 499
Exon 17	DNA 2	DNA 3	DNA 23	DNA 50	DNA 392				
Exon 19	DNA 2	DNA 3	DNA 6	DNA 392					
Exon 20	DNA 2	DNA 3	DNA 392	DNA 495					

Table 9. DNA sequencing results and confirmed genotypes for each exon. Samples highlighted in green were confirmed to be wild-type for that assay. Samples highlighted in yellow were confirmed heterozygous mutations. The DNA sample highlighted in red was a confirmed homozygous mutant.

Exon	Mutation	dbSNP/ESP	Tested (n=30)
2	c.128 G>A	7.70%	3.33%
8	c.663 C>T	0.50%	3.33%
8	c.623-8 C>T	0.01%	3.33%
15	c.1532+11 G>A	0.01%	3.33%
16	c.1605+6 T>C	49.00%	50.00%
16	c.1600 G>A	2.10%	3.33%
16*	c.1605+6 T>C	22.50%	36.70%

Table 10. The average frequency of each mutation as reported by the dbSNP or ESP database and the mutation frequency calculated from the blinded study. The frequencies reported by the dbSNP and ESP databases represent the average heterozygosity.

*This was the only homozygous mutation detected.

CHAPTER IV

DISCUSSION

The focus of this thesis was on the development of the *ACADVL* gene scanning assay

using a two-step PCR coupled with high resolution melting (HRM) analysis. We were able to

genotype 19 exons on the Light Cycler 480 using synthetic constructs and HRM as the analytical

method of detection. All heterozygote and 11 out of 18 homozygote mutations were detectable in

the CULS buffer system for the following exons: 1, 5, 6, 8, 11, 12, 13, 15, 17, 19, and 20. When

the PCR chemistry changed to the AT buffer, all heterozygote mutations were once again

detectable, but we were only able to detect 9 of the 19 homozygote plasmid DNA mutants

(Exons 2, 5, 6, 8, 9, 10, 11, 15, and 16). The inability to detect all homozygous mutations in a

scanning assay is a known phenomenon. Palais et al. (2005) explains an alternative approach to

homozygote detection by quantitative heteroduplex analysis using high resolution melting. In his

study, he added a known wild-type sample to samples with all three genotypes. Heteroduplexes

formed when wild-type DNA was added to homozygous and heterozygous mutants. The number

of heteroduplexes that formed depended on the genotype of the unknown sample and the fraction

of wild-type DNA added (Palais, et al., 2005). The difference between the melting curve of the

wild-type and the melting curve of the mutant was enhanced when wild-type DNA was added to

homozygous samples. The opposite was true when wild-type DNA was added to heterozygous

samples. According to Olsen et al. (2010), since homozygous detection depends on small

differences in T_m between alternative genotypes, it is especially sensitive to variations in sample

chemistry (Olsen, et al., 2010). This could explain the decrease in homozygote detection we saw

when the PCR chemistry changed to the AT buffer. Unfortunately, we were unable to produce

successful PCR results for exon 18. Numerous primer pairs were designed and tested on the

Light Cycler 480, but we were still unable to optimize this assay. Even though we were unable to

deduce the reason behind the inefficiency of the exon 18 assay, the preliminary data revealed that

the primers were amplifying other unknown targets.

After PCR efficiency was established, we performed a blinded study with 30 different

genomic DNA samples that were selected at random. Since a true wild-type genomic DNA was

not known for the *ACADVL* gene, synthetic constructs were used as controls. Samples with a

relative fluorescence difference of +/- 1.0 or greater were sent for sequencing. This was a very

conservative cut-off value, and we knew to expect many wild-type sequences returned. We

selected samples from each cluster, including those that appeared to be wild-type, and sent them

to Macrogen for purification and sequencing. Sequencing results proved that the selection

criteria we chose was indeed appropriate. Samples with relative fluorescence difference values

within +/- 1.0 range were wild-type whereas those with relative fluorescence difference values

outside these boundaries were found to harbor mutations (**Table 9**). A total of seven mutations

were detected with HRM, and these samples were confirmed by DNA sequencing (**Table 10).**

All seven mutations were non-pathogenic single nucleotide polymorphisms (SNPs) that had been

previously reported in either the Single Nucleotide Polymorphism database (dbSNP) or the

Exome Sequencing Project database (ESP). The heterozygous mutation for exon 2, c.128G>A, is

a non-synonymous substitution that changes amino acid glycine to a glutamic acid residue. Four

of the mutations (homozygous and heterozygous c.1605+11T>C, heterozygous c.623-8C>T and

heterozygous c.1532+11G>A) are non-coding substitutions that do not affect the amino acid

sequence. The heterozygous mutation found at position c.1600G>A on exon 16 is a non-

synonymous substitution that changes amino acid glutamic acid to a lysine residue. Heterozygous mutation c.663C>T is synonymous base substitution that does not alter the amino acid produced. The reported frequencies for each of these mutations were compared to the frequencies calculated based on our set of experiments (**Table 10**). The calculated frequencies were very similar to the expected frequency for each mutation as reported in the dbSNP or ESP databases.

HRM is the only scanning method that does not require physical processing or separation steps after amplification. The popularity of this analytical method is growing rapidly because of its simplicity (Erali & Wittwer, 2010). By removing the need for sample transfer, the risk of post-PCR manipulation and contamination is significantly reduced. Due to its speed and accuracy, this method could also substitute current metabolic testing. The data presented in this thesis supports the development of 19 out of 20 *ACADVL* scanning assays on the Light Cycler 480 and the sensitivity of the HRM technique for mutation detection within this gene. To bring this assay to clinical implementation, the following steps would be required: re-design, homozygote detection, clinical samples and clinical trials.

High resolution melting for gene scanning relies heavily on PCR quality, so optimization is critical. The current assay design outlined in this thesis requires different PCR cycling conditions for each exon. To move this assay to towards clinical implementation, we would need further optimization of the PCR protocol is needed. Efficient PCR results were not obtained for exon 18. The primers require re-design so the ACADVL scanning assay encompasses all 20 exons.

Gene scanning relies heavily on detecting heterozygous mutants by shape differences in the melting curves (Erali & Wittwer, 2010). Since homozygous variants rely on temperature differences (T_m), it is difficult to observe these differences through gene scanning. Homozygous variants are best detected by mixing a normal and unknown DNA samples together so any homozygotes in the unknown will form heteroduplexes (Erali & Wittwer, 2010). This would improve our ability to detect homozygous variants in the *ACADVL*.

In this thesis, I demonstrated the feasibility of the *VLCAD* scanning assay using a fast PCR protocol and HRM analysis of different mutations in the gene. I successfully optimized the assay in multiple PCR chemistries and demonstrated that it could be transferred to a microfluidic platform. In conclusion, HRM proved to be a fast and accurate analytical tool available for molecular diagnostics. The method introduced in this study can potentially be utilized for molecular genetic testing of any inherited metabolic disorder.

CHAPTER V

APPENDIX
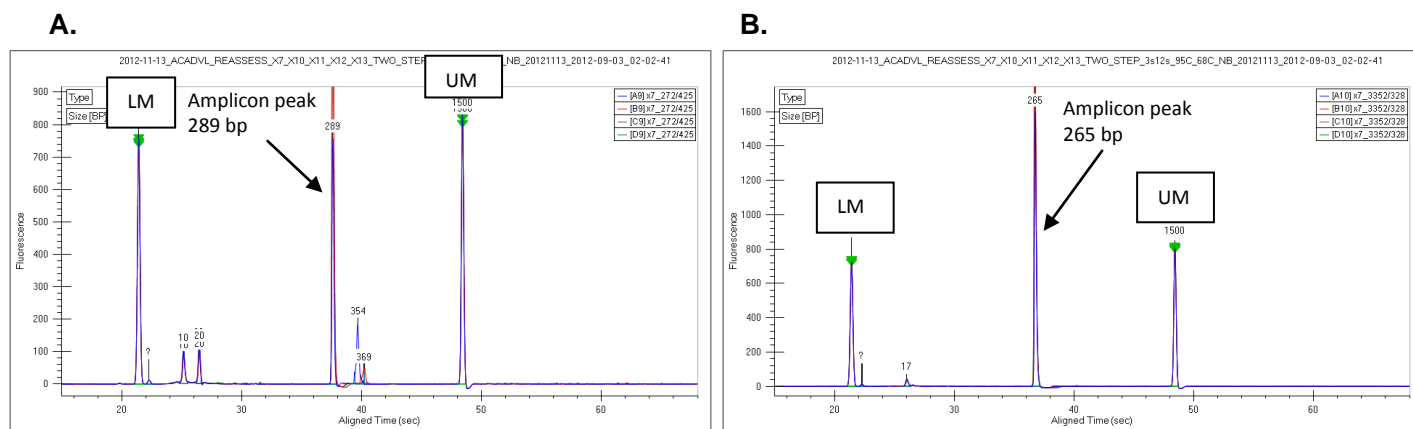
Figure 4. Two examples of Caliper GX-generated electropherograms pertaining to the PCR products for *ACADVL* exon 7. Genomic DNA was used as the template in both cases. Shown is a lower molecular weight marker (LM) and upper molecular weight marker (UM) in each image. The size of each amplicon is depicted in each graph as well. Electropherogram (A) is a Caliper GX image of primer pair 272/425. The larger peaks (354 bp and 359 bp) represent secondary products formed during amplification. Electropherogram (B) is a Caliper GX image of primer pair 3352/328. Only one band of the appropriate size (98% purity) was present in each well. This primer pair was chosen for genotyping.
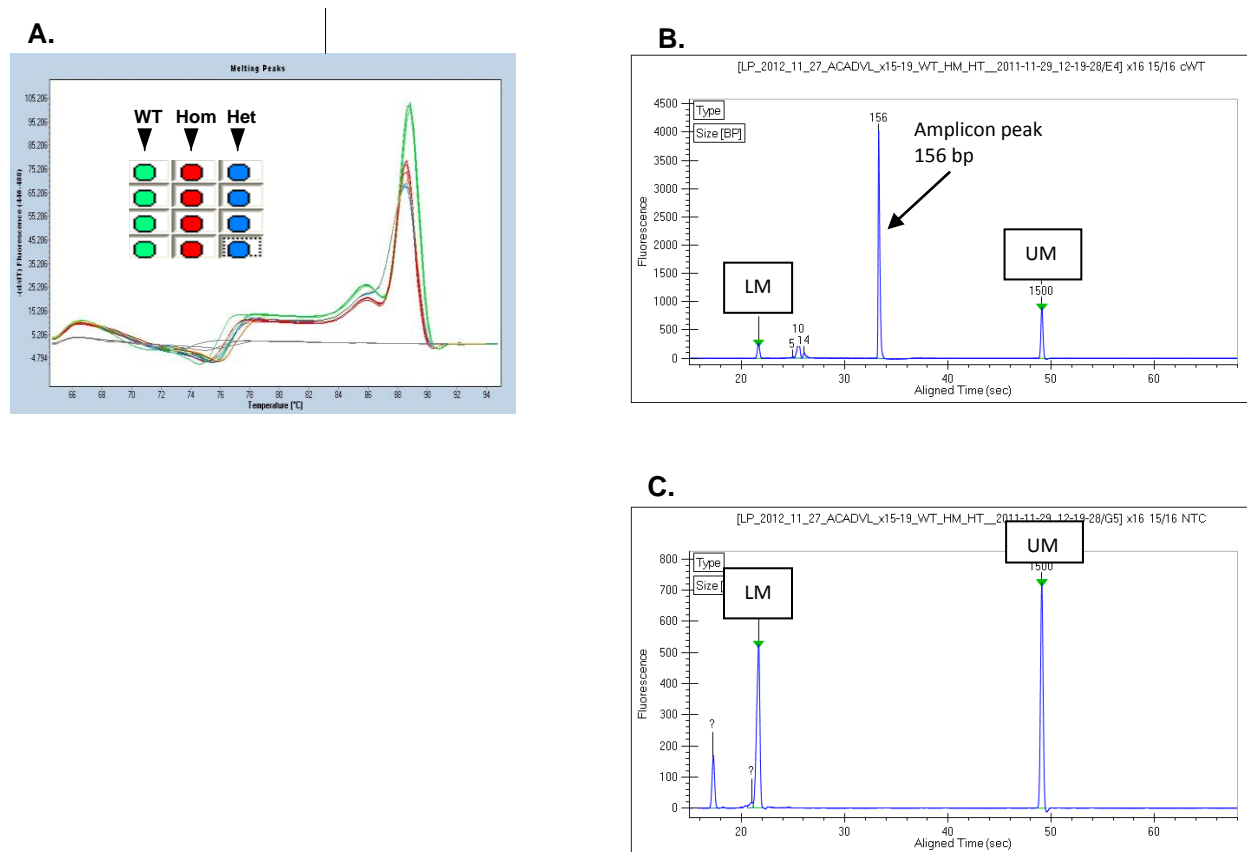
Figure 5. Derivative plot pertaining to exon 16 amplicon using pDNA as template (A), and Caliper GX electropherograms for wild-type amplicon (B) and NTCs (C). Shown is a lower molecular weight marker (LM) and upper molecular weight marker (UM) in each electropherogram. The amplicon peak (B) was the appropriate size for exon 16 (156 bp), with a purity >96%. The NTC electropherogram (C) does not show any peaks between the lower and upper molecular weight markers. This indicates that no secondary products formed during amplification of exon 16.
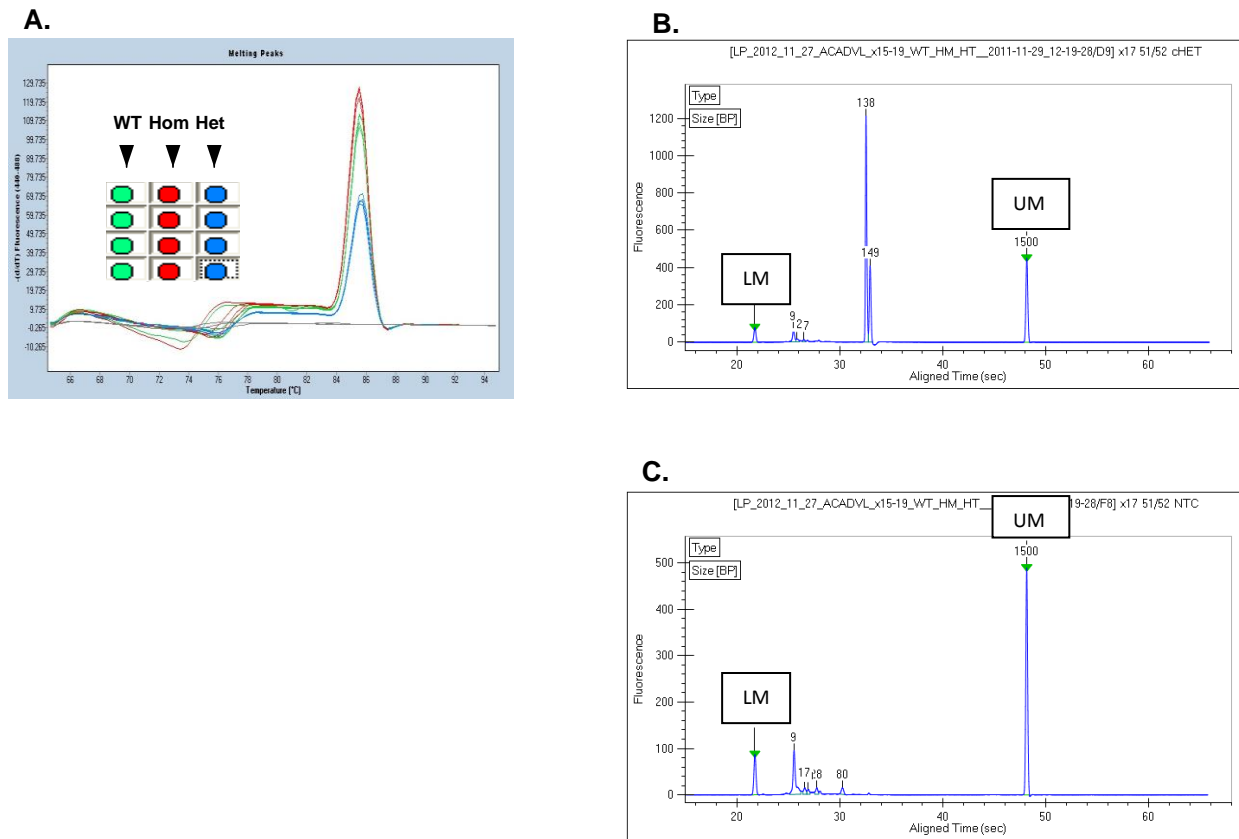
Figure 6. Derivative plot pertaining to exon 17 amplicon using pDNA as template (A), and Caliper GX electropherograms for heterozygote amplicon (B) and NTCs (C). There is a lower molecular weight marker (LM) and upper molecular weight marker (UM) in each electropherogram. Two PCR products of similar size are present in the heterozygote amplicon (B). Smaller peaks are present in the NTCs (C) that do not represent the desired product. The peaks could be a result of left over primers from the PCR reaction.
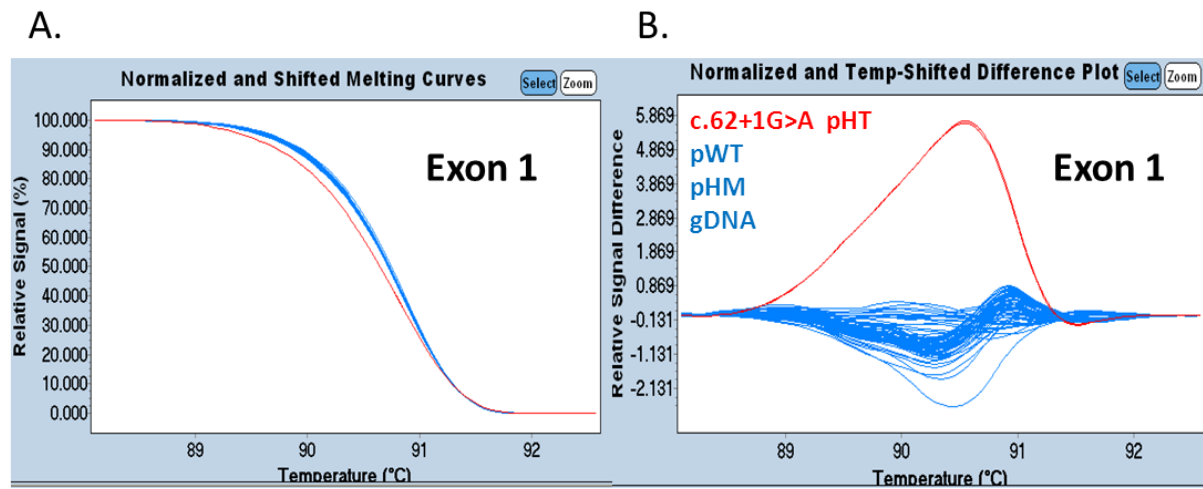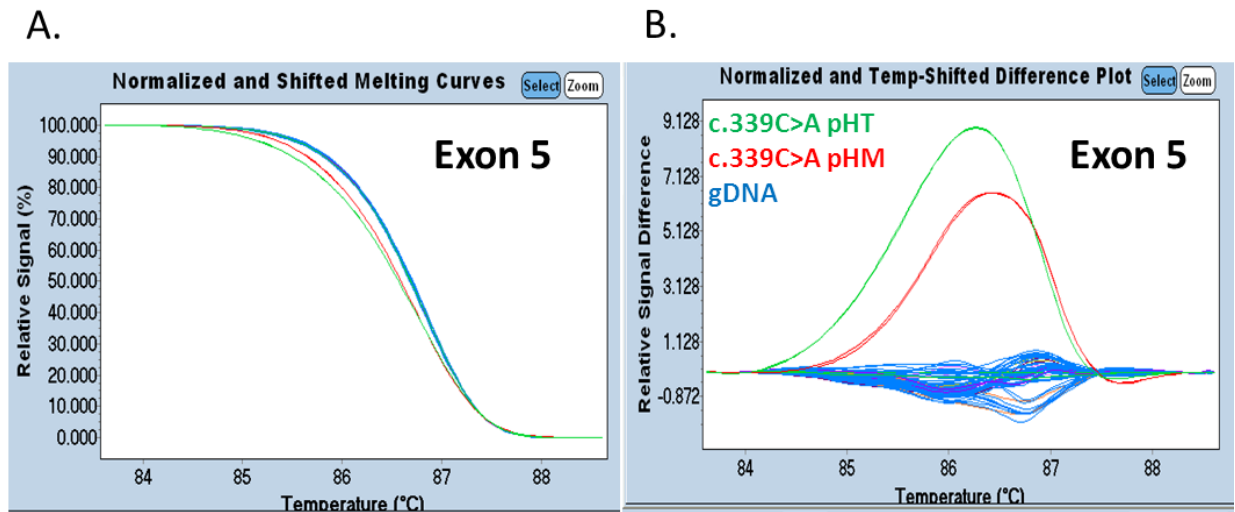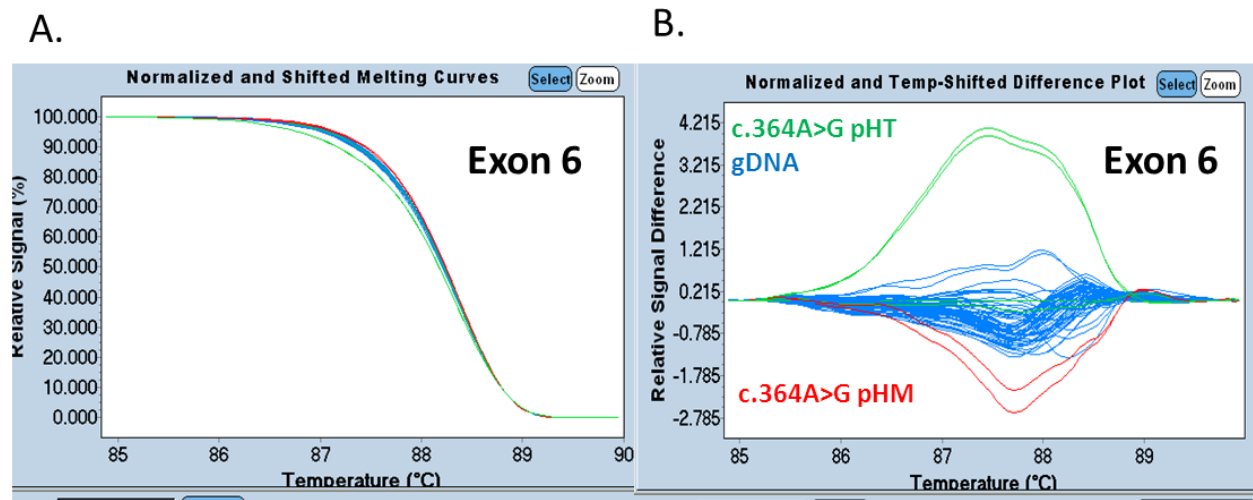
Figure 8. Summary of *ACADVL* exon 1 HRM scanning results. Normalized HRM curve (A) and difference plot (B) for Exon 1 blinded experiments. The difference plot shows 2 distinct groups (blue and red). The sample colors were provided by the Light Cycler 480 Gene Scanning software.
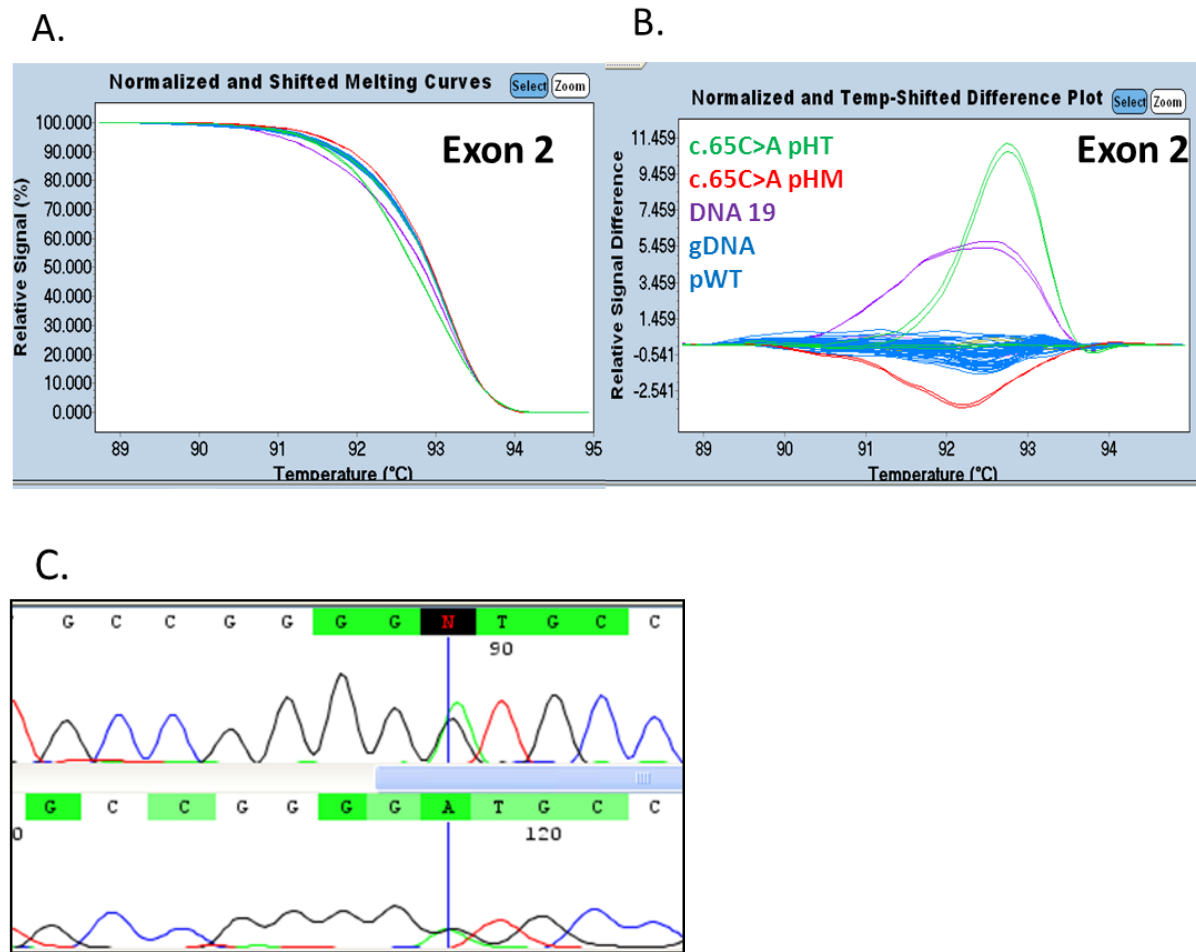
Figure 9. Summary of *ACADVL* exon 2 HRM scanning and sequencing results. Normalized

HRM curve (A) and difference plot (B) and sequencing results (C) for Exon 2 blinded

experiments with 30 randomly selected genomic DNA samples from. The difference plot shows

4 distinct groups: green, red purple, and blue. Sequencing results from Macrogen show the
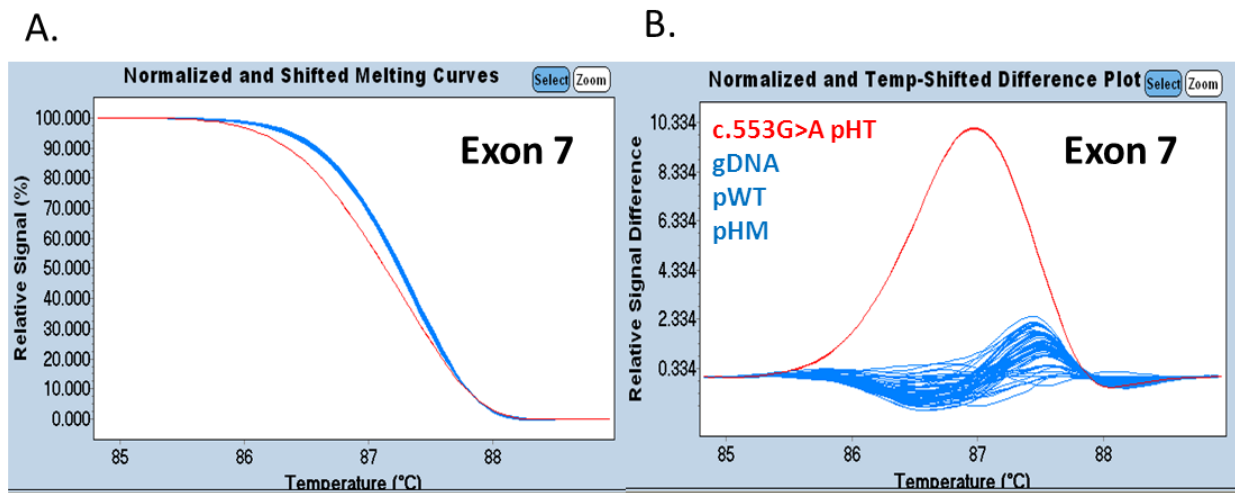
presence of a heterozygote mutation: c.128A>G.
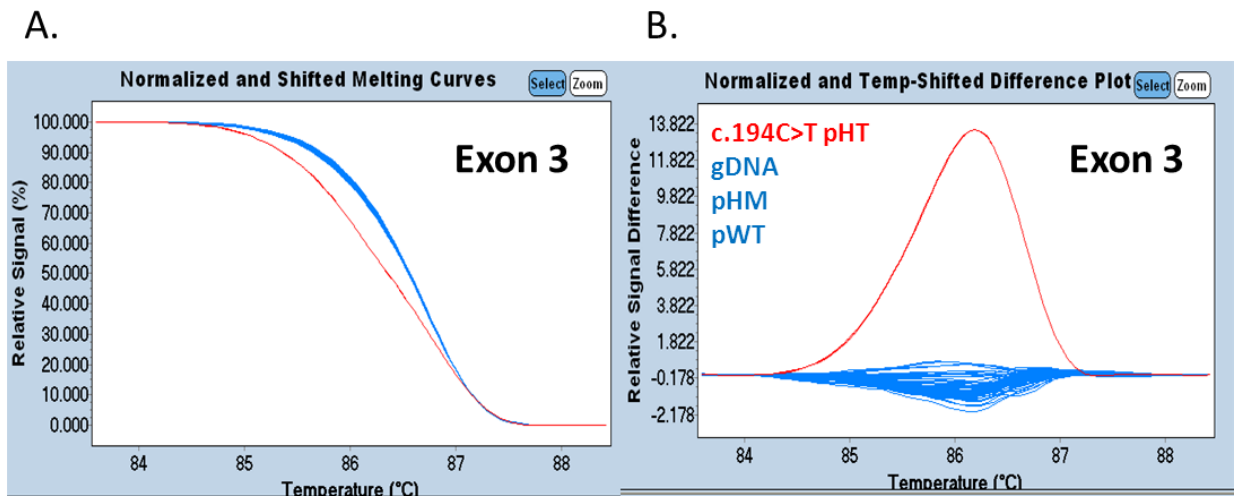
Figure 10. Summary of *ACADVL* exon 3 HRM scanning results. Normalized HRM curve (A) and difference plot (B) of Exon 3 blinded experiments with 30 randomly selected genomic DNA samples. The difference plot shows 2 distinct groups: blue and red. The sample colors were assigned by Light Cycler 480 Gene Scanning software.
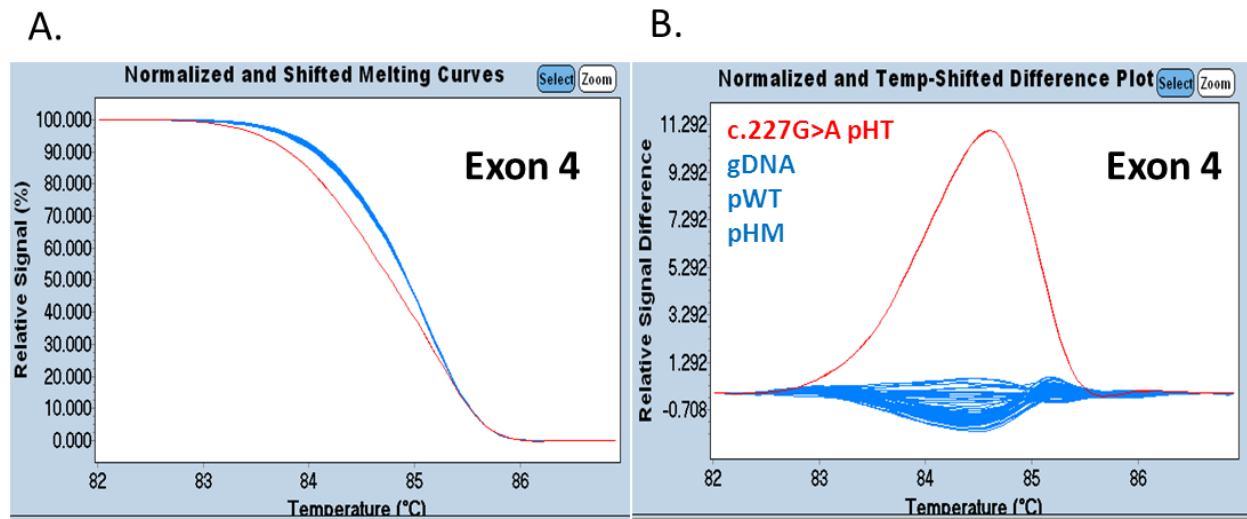
Figure 11. Summary of *ACADVL* exon 4 HRM scanning results. Normalized HRM curve (A) and difference plot (B) of Exon 4 blinded experiments with 30 randomly selected genomic DNA samples. The difference plot shows 2 distinct groups: blue and red. The sample colors were assigned by Light Cycler 480 Gene Scanning software.
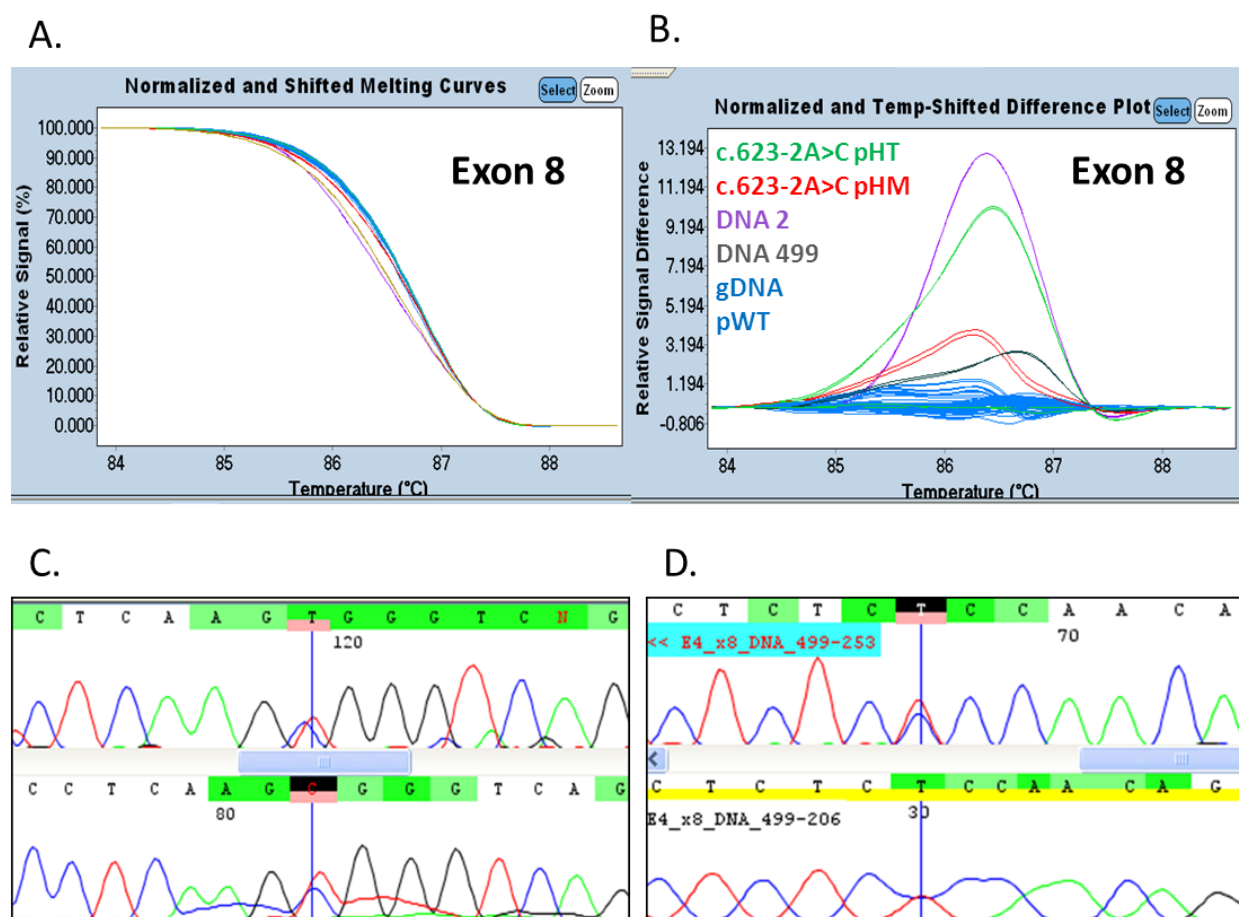
Figure 12. Summary of *ACADVL* exon 5 HRM scanning results. Normalized HRM curve (A) and difference plot (B) of Exon 5 blinded experiments with 30 randomly selected genomic DNA samples. The difference plot shows 3 distinct groups: blue, red, and green. The sample colors were manually assigned.

Figure 13. Summary of *ACADVL* exon 6 HRM scanning results. Normalized HRM curve (A) and difference plot (B) of Exon 6 blinded experiments with 30 randomly selected genomic DNA samples. The difference plot shows 3 distinct groups: blue, red, and green. The sample colors were manually assigned.
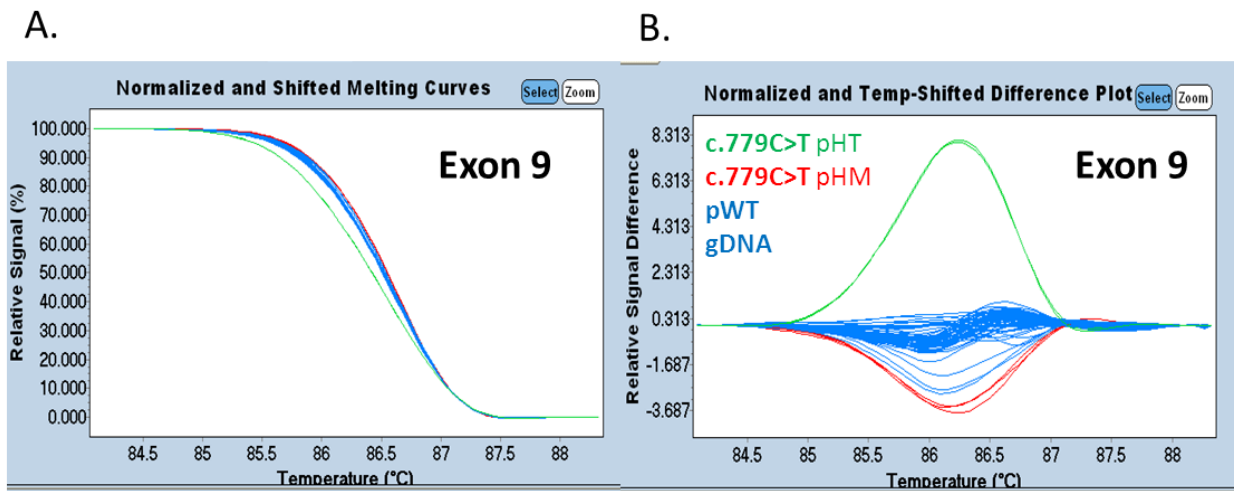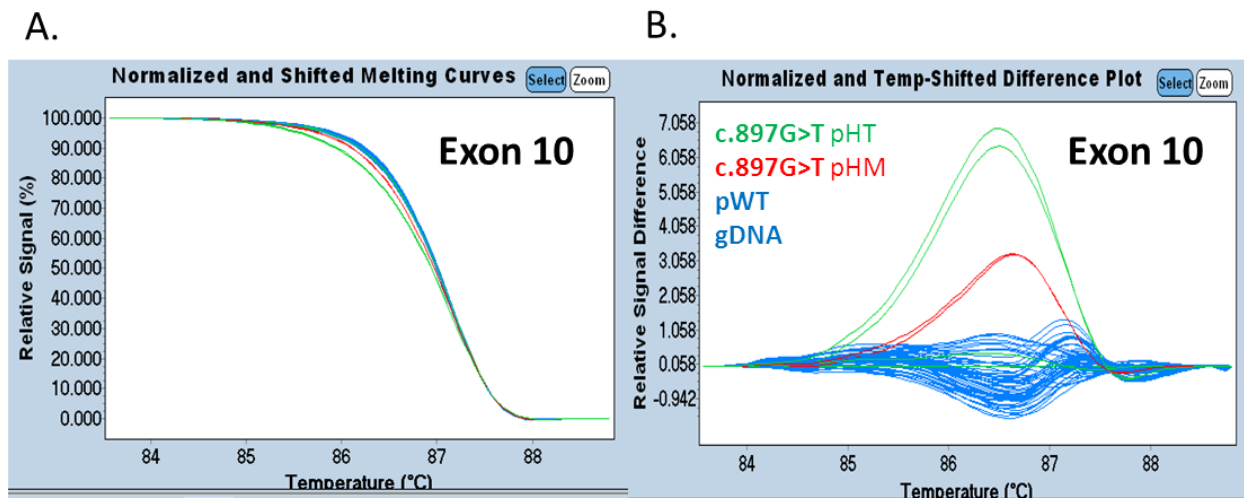
Figure 14. Summary of *ACADVL* exon 7 HRM scanning results. Normalized HRM curve (A) and difference plot (B) of Exon 7 blinded experiments with 30 randomly selected genomic DNA samples. The difference plot shows 2 distinct groups: blue and red. The sample colors were assigned by Light Cycler 480 Gene Scanning software.

Figure 15. Summary of *ACADVL* exon 8 HRM scanning and sequencing results.

Normalized HRM curve (A) and difference plot (B) and sequencing results (C), (D) of Exon 8

blinded experiments with 30 randomly selected genomic DNA samples. The difference plot

shows 4 distinct groups: blue, red, green, purple and black. The sample colors were manually

assigned. The sequencing results (C) confirmed the presence of a heterozygous mutation:

c.663C>T. The sequencing results (D) confirmed the presence of a heterozygous mutation:

c.623-8C>T.

Figure 16. Summary of *ACADVL* exon 9 HRM scanning results. Normalized HRM curve (A) and difference plot (B) of Exon 9 blinded experiments with 30 randomly selected genomic DNA samples. The difference plot shows 2 distinct groups: blue and red. The sample colors were manually assigned.
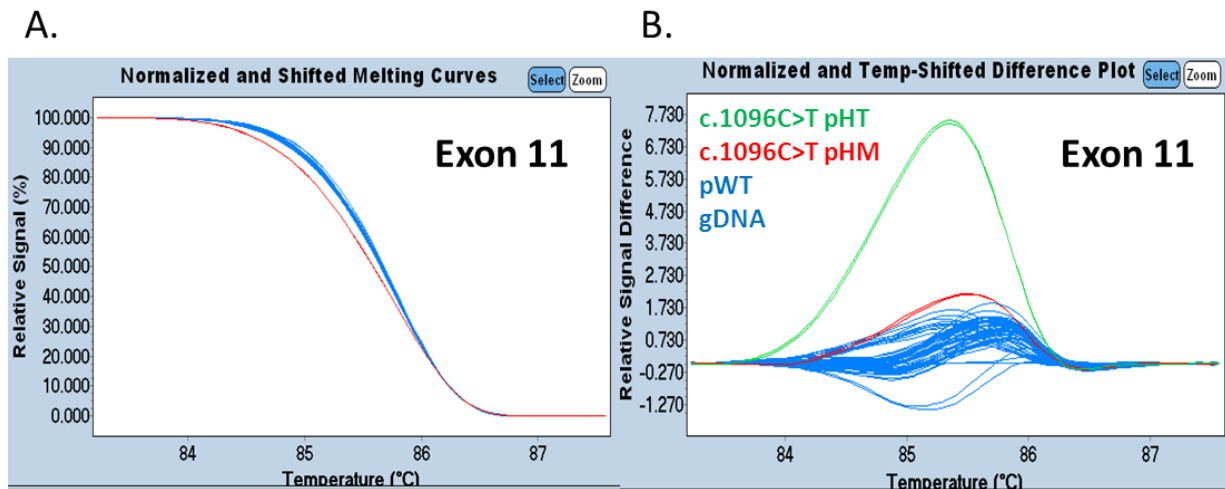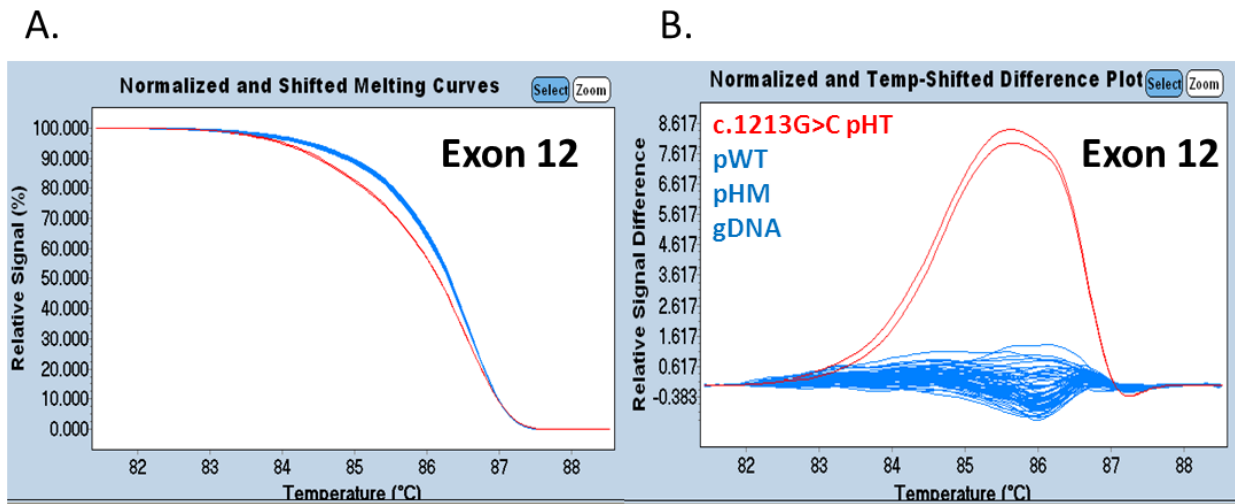
Figure 17. Summary of *ACADVL* exon 10 HRM scanning results. Normalized HRM curve

(A) and difference plot (B) of Exon 10 blinded experiments with 30 randomly selected genomic

DNA samples. The difference plot shows 2 distinct groups: blue and red. The sample colors were

manually assigned.

Figure 18. Summary of *ACADVL* exon 11 HRM scanning results. Normalized HRM curve (A) and difference plot (B) of exon 11 blinded experiments with 30 randomly selected genomic DNA samples. The difference plot shows 3 distinct groups: blue, red, and green. The sample colors were manually assigned.

Figure 19. Summary of *ACADVL* exon 12 HRM scanning results. Normalized HRM curve

(A) and difference plot (B) of exon 12 blinded experiments with 30 randomly selected genomic

DNA samples. The difference plot shows 2 distinct groups: blue and red. The sample colors were

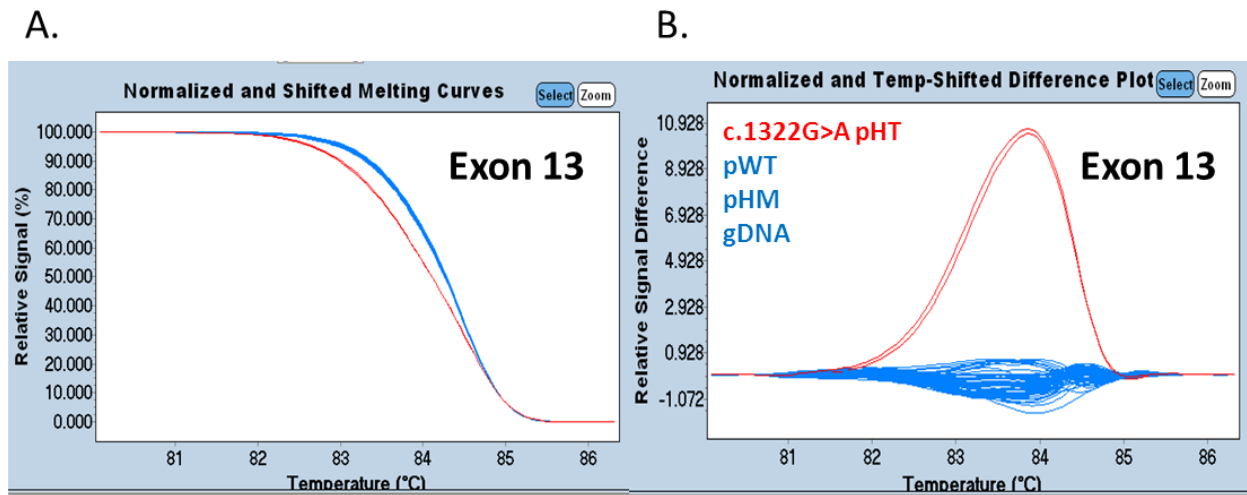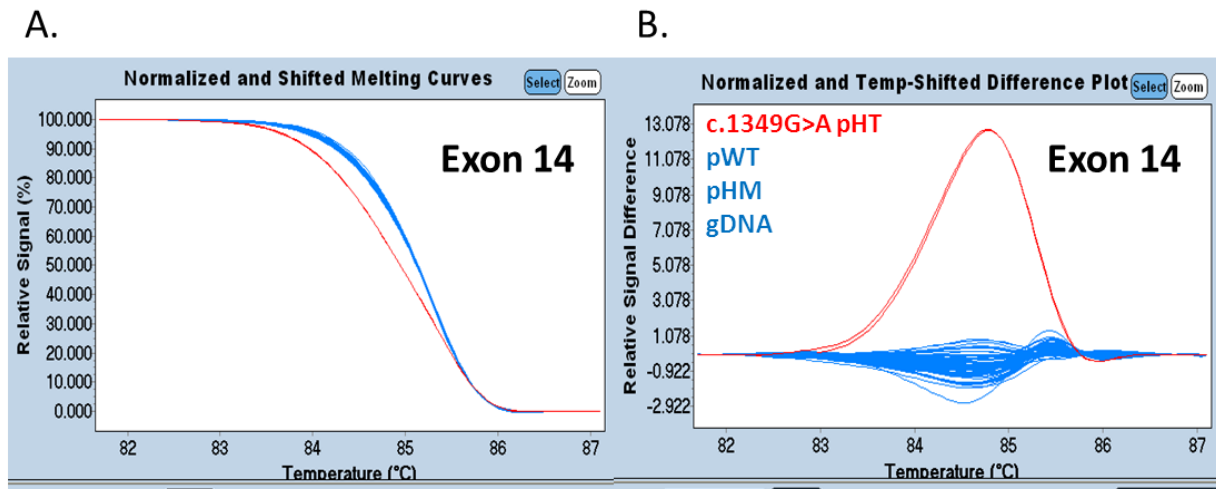assigned by Light Cycler 480 Gene Scanning software.

Figure 20. Summary of *ACADVL* exon 13 HRM scanning results. Normalized HRM curve (A) and difference plot (B) of exon 13 blinded experiments with 30 randomly selected genomic DNA samples. The difference plot shows 2 distinct groups: blue and red. The sample colors were assigned by Light Cycler 480 Gene Scanning software.

Figure 21. Summary of *ACADVL* exon 14 HRM scanning results. Normalized HRM curve

(A) and difference plot (B) of exon 14 blinded experiments with 30 randomly selected genomic

DNA samples. The difference plot shows 2 distinct groups: blue and red. The sample colors were

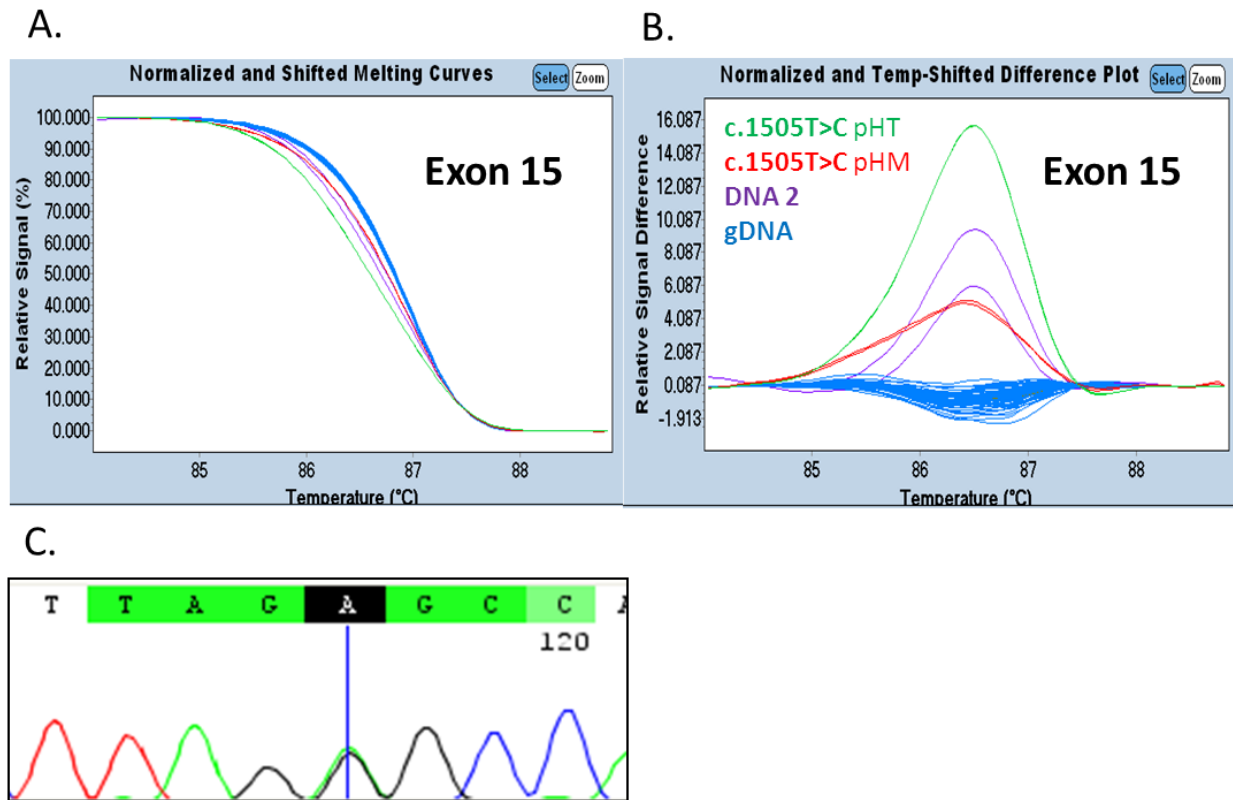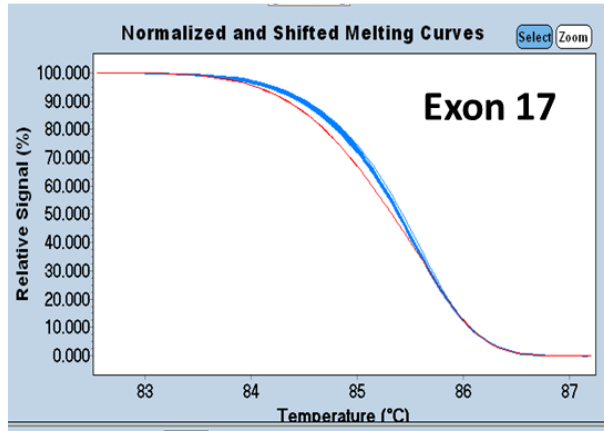assigned by Light Cycler 480 Gene Scanning software.

Figure 22. Summary of *ACADVL* exon 15 HRM scanning and sequencing results.

Normalized HRM curve (A), difference plot (B) and sequencing results (C) from Exon 15

blinded experiments with 30 randomly selected genomic DNA samples. The difference plot

shows 4 distinct groups: blue, red, green, and purple. The sample colors were manually assigned.

The sequencing results (C) confirmed the presence of a heterozygous mutation: c.1532+11G>A.
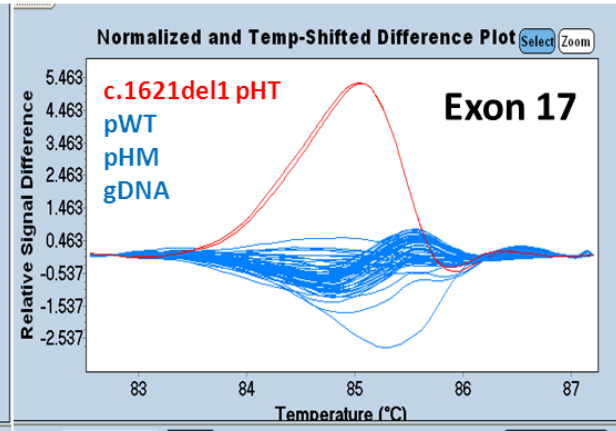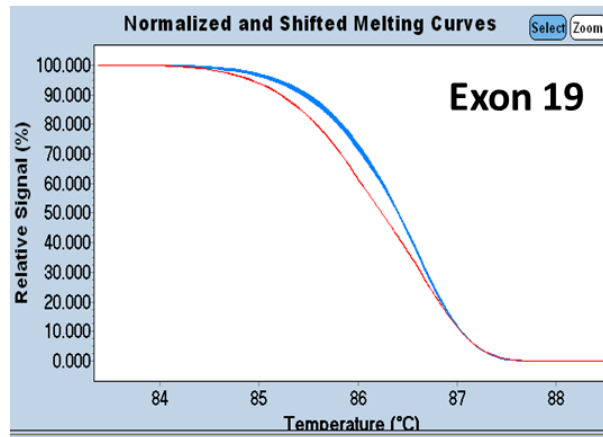
Figure 23. Summary of *ACADVL* exon 17 HRM scanning results. Normalized HRM curve

(A) and difference plot (B) of exon 17 blinded experiments with 30 randomly selected genomic

DNA samples. The difference plot shows 2 distinct groups: blue and red. The sample colors were

assigned by Light Cycler 480 Gene Scanning software.

A.

Normalized and Shifted Melting Curves [Select] [Zoom]

Exon 19

B.

Normalized and Temp-Shifted Difference Plot [Select] [Zoom]

c.1824C>T pHT
gDNA
pWT
pHM

Exon 19

Figure 24. Summary of *ACADVL* exon 19 HRM scanning results. Normalized HRM curve (A) and difference plot (B) of Exon 19 blinded experiments with 30 randomly selected genomic DNA samples. The difference plot shows 2 distinct groups: blue and red. The sample colors were assigned by Light Cycler 480 Gene Scanning software.
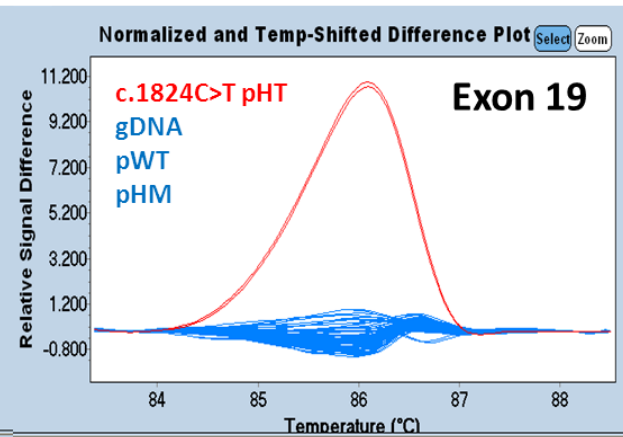
Figure 25. Summary of *ACADVL* exon 20 HRM scanning results. Normalized HRM curve (A) and difference plot (B) of exon 20 blinded experiments with 30 randomly selected genomic DNA samples. The difference plot shows 2 distinct groups: blue and red. The sample colors were assigned by Light Cycler 480 Gene Scanning software.
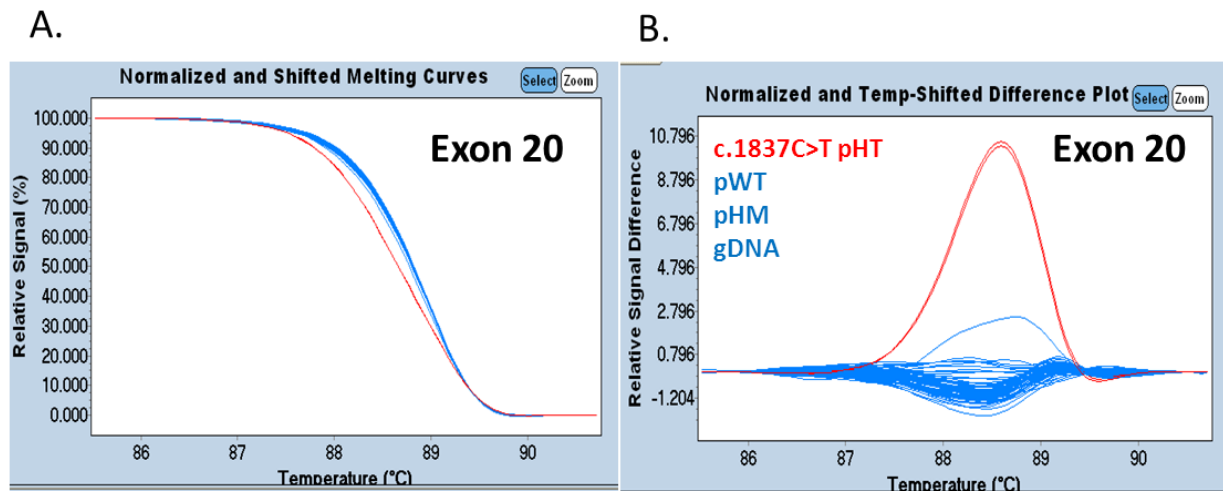
LITERATURE CITED

HRM. (2007). Retrieved February 2014, from Gene Quantification: http://hrm.gene-quantification.info/

Andresen, B., Olpin, S., Poorthuis, B., Scholte, H., Vianey-Saban, C., Wanders, R., et al. (1999). Clear Correlation of Genotype with Disease Phenotype in Very–Long-Chain Acyl-CoA Dehydrogenase Deficiency. *American Journal of Human GEnetics*, 479-494.

Benkhadra, N., Papazisi, L., & Huuskonen, J. (2013). *ACADVL Scanning Feasibility on LC480.* Rockville: Canon US Life Sciences, Inc.

Cox, et al. (2008). Reversal of severe hypertrophic cardiomyopathy and excellent neuropsychological outcome in very-long-chain acyl-coenzyme A dehydrogenase deficiency. *Journal of Pediatrics*, 247-253.

Croston, G. (2001, March). *Beta-Oxidation of Fatty Acids*. Retrieved February 2014, from Biocarta: http://www.biocarta.com/pathfiles/betaoxidationpathway.asp

Dames, et al. (2007). Characterization of Aberrant Melting Peaks in Unlabeled Probe Assays. *Journal of Molecular Diagnostics*, 290-296.

Erali, et al. (2008). High resolution melting applications for clinical laboratory medicine. *Experimental and Molecular Pathology*, 50-58.

Erali, et al. (2010). High resolution melting analysis for gene scanning. *Methods*, 250-261.

Goetzman, et al. (2007). EXPRESSION AND CHARACTERIZATION OF MUTATIONS IN HUMAN VERY LONG-CHAIN ACYL-COA DEHYDROGENASE USING A PROKARYOTIC SYSTEM. *Molecular Genetic Metabolism*, 138-147.

illumina. (2011). *An Introduction to Next-Generation Sequencing Technology.* Retrieved March 2014, from illumina: http://res.illumina.com/documents/products/illumina_sequencing_introduction.pdf

Leslie, et al. (2011). Very-Long-Chain Acyl-Coenzyme A Dehydrogenase Deficiency. *Gene Reviews*.

Liew, et al. (2004). Genotyping of Single-Nucleotide Polymorphisms by High-Resolution Melting of Small Amplicons. *Molecular Diagnostics and Genetics*, 1156-1164.

Liew, et al. (2007). Closed-Tube SNP Genotyping Without Labeled Probes. *American Journal of Clinical Pathology*, 341-348.

Liew, et al. (2007). Closed-Tube SNP Genotyping Without Labeled Probes. *American Journal for Clinical Pathology*, 341-348.

Matern, et al. (2012, January 19). *Medium-Chain Acyl-Coenzyme A Dehydrogenase Deficiency.* Retrieved March 2014, from NCBI GeneReviews: http://www.ncbi.nlm.nih.gov/books/NBK1424/

Miesfeld. (2008). *Lecture 34 - Fatty acid oxidation.* Retrieved February 2014, from http://www.biochem.arizona.edu/miesfeld/Miesfeld-Fall2008Lecs/Lec34-Fall08/Lec34-F08-Handout.pdf

Olsen, R., Dobrowolski, S., Kjeldsen, M., Hougaard, D., Simonsen, H., Gregersen, N., et al. (2010). High-resolution melting analysis, a simple and effective method for reliable mutation scanning and frequency studies in the ACADVL gene. *Journal of Inherited Metabolic Disorders*, 247-260.

Palais, et al. (2005). Quantitative heteroduplex analysis for single nucleotide polymorphism genotyping. *Analytical Biochemistry*, 167-175.

Reed, e. a. (2004). Sensitivity and Specificity of Single-Nucleotide Polymorphism Scanning by High-Resolution Melting Analysis. *Molecular Diagnostics and Genetics*, 1748-1754.

Reed, et al. (2007). High-resolution DNA melting analysis for simple and efficient molecular diagnostics. *Pharmacogenomics*, 597-608.

Ririe, et al. (1997). Product Differentiation by Analysis of DNA Melting Curves during Polymerase Chain Reaction. *Analytical Biochemistry*, 154-160.

SantaLucia Jr., J. (2007). Physical Principles and Visual-OMP Software for Optimal PCR Design. In J. John SantaLucia, *Methods in Molecular Biology, vol. 402: PCR Primer Design* (pp. 1-33). Totowa, NJ: Humana Press.

Schiff, et al. (2013). Molecular and cellular pathology of very-long-chain acyl-CoA dehydrogenase deficiency. *Molecular Genetics and Metabolism*, 21-27.

Schymik, I., Liebig, M., Mueller, M., Wendel, U., Mayatepek, E., Strauss, A., et al. (2006). PITFALLS OF NEONATAL SCREENING FOR VERY-LONG-CHAIN ACYL-COA DEHYDROGENASE DEFICIENCY USING TANDEM MASS SPECTROMETRY. *The Journal of Pediatrics*, 128-130.

Tein, I. (2002). Role of Carnitine and Fatty Acid Oxidation and Its Defects in Infantile Epilepsy. *Journal of Child Neurology*, 3S57-3S83.

Watson, et al. (2006). Newborn Screening: Toward a Uniform Screening Panel and System. *Official Journal of the American College of Medical Genetics*, 1S-11S.

Wittwer, C. T. (2010). Making DNA Melting Useful. *Clinical Chemistry*, 1500-1501.

CURRICULUM VITAE

Education

Master of Science in Forensic Science   May 2014
Towson University   Towson, MD

Bachelor of Science in Biochemistry, Minor in Chemistry   December 2010
Virginia Polytechnic Institute and State University (Virginia Tech)   Blacksburg, VA

Experience

Associate Scientist

Canon U.S. Life Sciences, Rockville, MD   March 2011-Present
- Designed PCR experiments for the *ACADVL* gene scanning assay.
- Performed DNA extractions from bacteria and blood using the Qiagen Qiacube and the Roche MagnaPure Compact instruments.
- Created and maintained a monthly budget for the Assay Development department.
- Trained personnel on proper lab safety.
- Wrote technical reports on projects completed.
- Wrote standard operating procedures.
- Assembled components for our prototype PCR and high resolution melting instrument.

Undergraduate Researcher

Biochemistry Department, Virginia Tech   September 2009 –May 2010
- Conducted research on *Arabidopsis* plants by varying environmental conditions and comparing wild-types and mutant forms.
- Performed experiments in which the effects of auxin, a plant growth hormone, were studied.
- Presented the research conducted to the lab in a power point presentation.

Laboratory Assistant

National Institute of Health, Bethesda MD   May – August 2007
- Successfully sub-cloned human Vps34 (a protein kinase) into a mammalian vector
- Transfected Vps34 into a cancer cell line in order to study its effects on vesicular trafficking within these cells.
- Well-trained in PCR procedures.

Relevant Training
- Blood Borne Pathogen
- Hazardous Communication
- First aid and fire safety